Received XX Month, XXXX; revised XX Month, XXXX; accepted XX Month, XXXX; Date of publication XX Month, XXXX; date of current version XX Month, XXXX.

Digital Object Identifier 10.1109/OJCOMS.2022.1234567

Received Power Maximization Using Nonuniform Discrete Phase Shifts for RISs With a Limited Phase Range

DOGAN KUTAY PEKCAN, GRADUATE STUDENT MEMBER, IEEE, HONGYI LIAO, GRADUATE STUDENT MEMBER, IEEE, AND ENDER AYANOGLU, FELLOW, IEEE

[1]Center for Pervasive Communications and Computing (CPCC), Department of Electrical Engineering and Computer Science, University of California, Irvine, Irvine, CA 92697 USA

CORRESPONDING AUTHOR: Ender Ayanoglu (e-mail: ayanoglu@uci.edu).

This work is partially supported by NSF grant 2030029.

ABSTRACT To maximize the received power at a user equipment, the problem of optimizing a reconfigurable intelligent surface (RIS) with a limited phase range and nonuniform discrete phase shifts with adjustable gains is addressed. Necessary and sufficient conditions to achieve this maximization are given. These conditions are employed in two algorithms to achieve the global optimum in linear time. Depending on the phase range limitation, it is shown that the global optimality is achieved in NK or fewer and $N(K+1)$ or fewer steps, where N is the number of RIS elements and K is the number of discrete phase shifts which may be placed nonuniformly over the limited phase range. In addition, we define two quantization algorithms that we call nonuniform polar quantization (NPQ) algorithm and extended nonuniform polar quantization (ENPQ) algorithm, where the latter is a novel quantization algorithm for RISs with a significant phase range restriction. With NPQ, we provide a closed-form solution for the approximation ratio with which an arbitrary set of nonuniform discrete phase shifts can approximate the continuous solution. We also show that with a phase range limitation, equal separation among the nonuniform discrete phase shifts maximizes the normalized performance. Furthermore, for a larger RIS phase range limitation, we show that the gain of increasing K is only marginal, whereas, ON/OFF selection for the RIS elements can bring significant performance compared to the case when the RIS elements are strictly ON.

INDEX TERMS Intelligent reflective surface (IRS), reconfigurable intelligent surface (RIS), nonuniform discrete phase shifts, IRS/RIS phase range, global optimum, linear time discrete beamforming for IRS/RIS, nonuniform quantization.

I. INTRODUCTION

A reconfigurable intelligent surface (RIS), also known as intelligent reflective surface (IRS) is proposed for wireless environments where there may be blockage of electromagnetic waves between the base station (BS) and user equipment (UE), creating a low line-of-sight (LOS) environment [1]. An RIS can also be employed to generate a wireless coexistence environment by avoiding an area which may have its own transmissions and transmitting to users in a different area via reflections. An RIS employs devices known as RIS elements whose capacitance can be changed by controlling their bias voltage, affecting the phase of the RIS element, thereby creating a change in the reflection coefficient of the RIS element. This results in changing the direction of an impingent electromagnetic wave [2]–[4]. Assuming the phase shifts at the RIS elements are continuous, optimization algorithms are developed, for example, [5]–[8].

A two-stage approach to address the discrete phase shifts constraints for the single-user system is to project the continuous solution to the closest value in the discrete set [9]–[12]. With discrete phase shifts constraints, the number of possible solutions increases exponentially with the number of RIS elements. Therefore, a closed-form solution becomes practically unavailable and exponential search techniques are

required [13]. To that end, [14] stated that the problem is a generally NP-hard discrete quadratic program (QP). Most of the prior work in single-user scenarios had exponential complexity [9], [15]. In this regard, to outperform the traditional quantization approach, probabilistic optimization techniques have also drawn attention [16]–[18]. To address multi-user detection in code division multiple access, the probabilistic data association (PDA) approach is used in [16] to address general binary quadratic problems (BPQs). Similarly, in [17], authors addressed BPQs with a PDA algorithm and achieved near-optimal results for highly reliable machine-to-machine communication. Recently, the authors in [18] showed the general quantization approaches can be outperformed in various discrete RIS optimization problems by developing a comprehensive probabilistic technique to transform discrete optimization problems. Yet, most of the solutions not only assume uniform discrete phase shifts but also can only approximate the global optimum.

There has been a significant amount of research activity for the selection of uniform discrete phases when the phase range is 2π, see e.g., references in [19]. However, the problem of the selection of discrete phases when the phase range is limited to less than 2π is new and there are only a few works that appeared in the literature or as preprints [20]–[22]. Reference [20] states a uniform phase shift assumption is not realistic according to the actual behavior of practical RIS elements. The paper maximizes the channel capacity of the target user. It claims to develop a method that finds the optimal reflection amplitudes and phases with complexity linear in the number of RIS elements. Reference [21] states it models reflection coefficients as discrete complex values that have nonuniform amplitudes and suffer from insufficient phase shift capability. It proposes a group-based query algorithm that takes the imperfect coefficients into consideration. The authors have fabricated an RIS prototype system and validate their theoretical results by experiments. Reference [22] recognizes that in real-world applications, the phase and bit resolution of RIS units are often nonuniform due to practical requirements and engineering challenges. The authors formulate an optimization problem for discrete nonuniform phase configuration in RIS-assisted multiple-input single-output (MISO) communications. They state they propose a partition-and-traversal algorithm which achieves the global optimal solution.

We note that the problem of a limited phase range can actually happen in a real RIS system. For example, a common technology to implement an RIS is to employ varactor diodes and change their capacitance via varying their bias voltages. The change in capacitance makes the reflection coefficient of the RIS element to change, thereby creating the desired effect via the RIS. However, in the implemented RIS element, the voltage changes may not correspond to the full range of $-\pi$ to π (or -180° to 180°). As an example, [4] discusses a prototype for an RIS implemented via varactor diodes. In [4, Fig. 3], it can be observed that for the frequency the RIS is designed to operate at, i.e., 5.8 GHz, the change in the phase of the reflection coefficient is restricted to -120° to 110°. At frequencies different than 5.8 GHz, the range is even smaller.

Our motivation in this paper is to address the discrete-phase RIS problem to maximize the received power at a UE with the particular emphasis that the phase range is less than 2π. As described above, this can occur commonly in realistic implementations of the RIS structure where the components that realize the phase change in an RIS element are varactor diodes. In these settings, it is possible that the algorithms developed for the full phase range of 2π will not work and thus new algorithms need to be developed. Inspired by our work in [19], we are also motivated to find out if intuitive suboptimal algorithms to solve this problem can be found. For example, is it possible to employ intuitive techniques that have an approach of quantization within the limited phase range? If yes, we would like to quantify how closely they can perform compared to the optimum solution. We are also motivated to find closed-form expressions as to the fundamental limits of such techniques. Another key motivation is optimizing the placement of discrete phase shifts, i.e., selecting the phase shift set. Previously, these were uniformly set based on the number of phases, but with the possibility of nonuniform phases, this requires analysis.

Our work in this paper provides, as an extension of the work in [19], necessary and sufficient conditions for global optimality, two algorithms to achieve the optimum solution which can have smaller number of steps than the works in the literature, and two intuitive quantization algorithms which achieve near-optimal performance with very small complexity. We provide fundamental limits for the quantization approach. We also show that the best solution for this approach is obtained when equal separation among the discrete phases in the limited phase range is achieved.

In quantitative terms, the contributions of the paper are as follows.

- To maximize the received power at a user equipment, the problem of optimizing an RIS with a limited phase range $R < 2\pi$ and nonuniform discrete phase shifts with adjustable gains is addressed and necessary and sufficient conditions to achieve this maximization are given.
- These conditions are employed in two novel algorithms to achieve the global optimum in *linear time* for $R \geq \pi$ and $R < \pi$. With a total number of $N(K+1)$ and $N(K+2)$ complex vector additions when $R \geq \pi$ and $R < \pi$, it is shown that the global optimality is achieved in NK or fewer and $N(K+1)$ or fewer steps, respectively, where N is the number of RIS elements and K is the number of discrete phase shifts. To the best of our knowledge, the required complexity is the lowest available in the literature.
- In addition, we define two quantization algorithms that we call nonuniform polar quantization (NPQ) algorithm and extended nonuniform polar quantization (ENPQ)

algorithm, where the latter is a novel quantization algorithm for RISs with a significant phase range restriction, i.e., $R < \pi$.
- With NPQ, we provide a closed-form solution for the approximation ratio with which an arbitrary set of nonuniform discrete phase shifts can approximate the continuous solution. With this, we analyze the optimal placement of the nonuniform discrete phases overseen by literature. We show that with a phase range limitation, equal separation among the nonuniform discrete phase shifts maximizes the normalized performance.
- Furthermore, we show that the gain of using more than two discrete phase shifts with $R < \pi/2$ and more than three discrete phase shifts with $R < \pi$ is only marginal, i.e., increasing the number of discrete phase shifts does not improve the performance when R is limited.
- Finally, we prove that when $R < 2\pi/3$, ON/OFF selection for the RIS elements brings significant performance compared to the case when the RIS elements are strictly ON.

The rest of this paper is organized as follows. Section II introduces the system model and the problem definition. With strictly ON RIS gains, an optimal algorithm and a suboptimal quantization algorithm are developed in Section III and Section IV, respectively. Based on the quantization algorithm, Section V provides an approximation ratio for the performance. With the approximation ratio, an analytical analysis for the optimum placement of discrete phases is provided in Section VI. Then the RIS gains are relaxed. Considering adjustable RIS gains, Section VII, Section VIII, and Section IX provide an optimal algorithm, a suboptimal algorithm, and an approximation ratio of the performance for $R < \pi$. Section X analyzes convergence to optimality. Performance and complexity analyses are provided in Section XI, in comparison with the recent literature. Section XII has a brief discussion on an extension to the multi-user scenario. Finally, Section XIII provides the conclusion of the paper.

II. SYSTEM MODEL

We consider a point-to-point communication scenario aided by an RIS with N elements and a phase range R. The RIS elements introduce a gain and a phase shift, i.e., β_n^r and θ_n for $n = 1, \ldots, N$, respectively, to the incident signal. We consider K discrete phase shifts for the RIS elements $\theta_n \in \Phi_K$, where $\Phi_K = \{\phi_1, \phi_2, \ldots, \phi_K\}$ and the RIS gains can be adjustable, i.e., $\beta_n^r \in [0, 1]$. We also define the difference among each adjacent phase shift in Φ_K as $\Omega_K = \{\omega_1, \omega_2, \ldots, \omega_K\}$, such that $\phi_{k\oplus 1} = \phi_k + \omega_k$[1]. Hence, the N-element reflection coefficient vector is

$$\mathbf{w} = \left[\beta_1^r e^{j\theta_1}, \beta_2^r e^{j\theta_2} \ldots, \beta_N^r e^{j\theta_N}\right] \tag{1}$$

where $j = \sqrt{-1}$. Let $s \in \mathbb{C}$ be the transmitted symbol. The received signal is given as [19]

$$y = (\mathbf{h}_u^T \mathbf{W} \mathbf{h}_b + h_0)s + z, \tag{2}$$

where $h_0 \in \mathbb{C}$ is the direct link between the BS and UE with non-line-of-sight (NLOS), $\mathbf{W} = \text{diag}(\mathbf{w})$, z is the additive white Gaussian noise (AWGN), $\mathbf{h}_u \in \mathbb{C}^{N\times 1}$ and $\mathbf{h}_b \in \mathbb{C}^{N\times 1}$ are the equivalent channels of the RIS-UE and BS-RIS links, respectively.

Let h_n be the complex-valued cascaded channel coefficient between the BS and the UE, being reflected by the nth RIS element, $n = 1, \ldots, N$, i.e., let $\mathbf{h} = \mathbf{h}_u \odot \mathbf{h}_b$, where $\odot$ is the elementwise (Hadamard) multiplication of the two vectors. Assuming a mean power constraint $\mathbb{E}[|s|^2] \leq P$ at the BS, the achievable ergodic data rate in bps/Hz is given by

$$\gamma = \mathbb{E}\left[\log\left(1 + \frac{P}{\sigma^2}\left|h_0 + \mathbf{h}^T\mathbf{w}\right|^2\right)\right], \tag{3}$$

where $z \sim \mathcal{CN}(0, \sigma^2)$ and σ^2 is the noise power.

The RIS aids the communication through discrete beamforming to maximize the overall channel gain in equation (3). In practical scenarios, RISs have a certain phase-shifting capability, and the discrete phase shifts are not necessarily uniform [23]. In this paper, the RIS phase range $R \in [0, 2\pi]$ represents the phase-shifting capability of the RIS. Hence, we assume that the main restriction arises due to the RIS phase range $R < 2\pi$, and the nonuniform phase shifts are selected based on the RIS phase range as in Fig. 1.

At this point, we would like to emphasize an important point regarding the placement of the limited phase range R on the unit circle. We remark that the symmetry between the phase shifts $-\frac{R}{2}$ and $\frac{R}{2}$ in Fig. 1 is not required and the techniques presented in this paper apply to any nonuniform discrete phase shifts structure with a total contiguous phase range R. Because, for an arbitrary nonuniform phase shift structure, the RIS phase range would satisfy the condition $R = 2\pi - \omega_{\bar{k}}$ where $\omega_{\bar{k}}$ is the largest value in the set Ω_K. So, without loss of generality, we will use the approach in Fig. 1, i.e., $-\pi \leq \phi_1 < \cdots < \phi_K = \phi_1 + R < \pi$ with $R < 2\pi\frac{K-1}{K}$. The condition $R < 2\pi\frac{K-1}{K}$ arises due to the fact that R comes from $\omega_{\bar{k}}$, and the condition $\omega_{\bar{k}} \geq \frac{2\pi}{K}$ must be satisfied as $\sum_{k=1}^{K} \omega_k = 2\pi$ and by its definition $\omega_{\bar{k}} \geq \omega_k$, for $k \in \{1, 2, \ldots, K\} \setminus \bar{k}$. Note that, this will ensure that the discrete phase shifts cannot be placed uniformly over the unit circle[2]. In addition, while we recognize the phase range is not necessarily symmetric, we will assume the discrete phase shifts to be distributed over the range $[-\frac{R}{2}, \frac{R}{2}]$, without loss of generality.

[1] In this paper, we define $\oplus$ and $\ominus$ to choose from RIS phase shift indexes from 1 to K as follows. For $k_1, k_2 \in \{1, \ldots, K\}$, $k_1 \oplus k_2 = k_1 + k_2$ if $k_1 + k_2 \leq K$ and $k_1 \oplus k_2 = k_1 + k_2 - K$, otherwise. Similarly, for $k_1, k_2 \in \{1, \ldots, K\}$, $k_1 \ominus k_2 = k_1 - k_2$ if $k_1 > k_2$ and $k_1 \ominus k_2 = K + k_1 - k_2$, otherwise.

[2] Note that the terms uniform and nonuniform depend on the range over which they are defined. In this paper, we use the term nonuniform to mean the distribution over the full phase range $[-\pi, \pi)$ is nonuniform, or not equally separated.

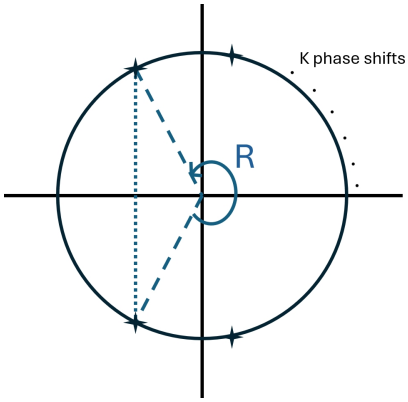

FIGURE 1: Nonuniform phase placement for $R \in [0, 2\pi]$.

A. PROBLEM DEFINITION

In this paper, we extend the problem of finding discrete phase shifts to maximize the received power at a UE for transmission, reflected by an RIS, originated from a BS, see, e.g., [19]. In particular, we address the problem of finding the values $\theta_1, \theta_2, \ldots, \theta_N$ and $\beta_1^r, \beta_2^r, \ldots, \beta_N^r$ to maximize the received power $\left|h_0 + \sum_{n=1}^N h_n \beta_n^r e^{j\theta_n}\right|^2$ in equation (3), or its square root, using nonuniform discrete phase shifts.

We would like to remind the reader that in $\left|h_0 + \sum_{n=1}^N h_n \beta_n^r e^{j\theta_n}\right|$, the values $h_n = \beta_n e^{j\alpha_n}$, $n = 0, 1, 2, \ldots, N$ are the channel coefficients and θ_n, $n = 1, 2, \ldots, N$ are the phase values added to the corresponding h_n by an RIS. As for the moment, we let $\beta_n^r = 1$, $n = 1, \ldots, N$, which we will relax after further analysis in this paper.

Initially, the problem can be formally described as

$$\begin{aligned} &\underset{\boldsymbol{\theta}}{\text{maximize}}\ f(\boldsymbol{\theta}) \\ &\text{subject to } \theta_n \in \Phi_K,\ n = 1, 2, \ldots, N \end{aligned} \tag{4}$$

where

$$f(\boldsymbol{\theta}) = \left|\beta_0 e^{j\alpha_0} + \sum_{n=1}^N \beta_n e^{j(\alpha_n + \theta_n)}\right|^2, \tag{5}$$

$\beta_n \geq 0$, $n = 0, 1, \ldots, N$, $\boldsymbol{\theta} = (\theta_1, \theta_2, \ldots, \theta_N)$, and $\alpha_n \in [-\pi, \pi)$ for $n = 0, 1, \ldots, N$.

We will provide optimal and suboptimal but computationally efficient algorithms for the problem. Furthermore, we will analyze the arbitrary phase shift placement and their optimality of approximating the continuous solution for large N, in regards to the RIS phase range.

In the next section, we will define our nonuniform discrete phase shift selection algorithm that guarantees the global optimal solution for $\beta_n^r = 1$, $n = 1, 2, \ldots, N$, or equivalently when $R \geq \pi$, and it will be an extension of [19, Algorithm 1]. We further improve it in the sequel by relaxing β_n^r in the interval $[0, 1]$ to improve the performance whenever the RIS phase range is less than π, i.e., $R < \pi$.

III. OPTIMAL SOLUTION WITH NONUNIFORM DISCRETE PHASE SHIFTS

In this section, we aim to solve the received power maximization problem, so that we can get the global optimum solution in linear time. We want to maximize $\left|h_0 + \sum_{n=1}^N h_n e^{j\theta_n}\right|$ where $h_n = \beta_n e^{j\alpha_n}$ for $n = 0, 1, \ldots, N$, and $\boldsymbol{\theta} = (\theta_1, \theta_2, \ldots, \theta_N)$. Define g as

$$g = h_0 + \sum_{n=1}^N h_n e^{j\theta_n^*} \tag{6}$$

where θ_n^* are the discrete phase shifts that lead to the global optimum. Let $\mu = g/|g|$ so that $|g| = ge^{(-j\angle\mu)}$. Similar to the condition in [19], we can make use of the following lemma.

Lemma 1: For an optimal solution $(\theta_1^*, \theta_2^*, \ldots, \theta_n^*)$, it is necessary and sufficient that each θ_n^* satisfy

$$\theta_n^* = \arg \max_{\theta_n \in \Phi_K} \cos(\theta_n + \alpha_n - \angle\mu) \tag{7}$$

for an arbitrary Φ_K.

Proof: We can rewrite $|g| = ge^{(-j\angle\mu)}$ as

$$\begin{aligned} |g| &= \beta_0 e^{j(\alpha_0 - \angle\mu)} + \sum_{n=1}^N \beta_n e^{j(\alpha_n + \theta_n^* - \angle\mu)} \\ &= \beta_0 \cos(\alpha_0 - \angle\mu) + j\beta_0 \sin(\alpha_0 - \angle\mu) \\ &\quad + \sum_{n=1}^N \beta_n \cos(\theta_n^* + \alpha_n - \angle\mu) \\ &\quad + j \sum_{n=1}^N \beta_n \sin(\theta_n^* + \alpha_n - \angle\mu). \end{aligned} \tag{8}$$

Because $|g|$ is real-valued, the second and fourth terms in (8) sum to zero, and

$$|g| = \beta_0 \cos(\alpha_0 - \angle\mu) + \sum_{n=1}^N \beta_n \cos(\theta_n^* + \alpha_n - \angle\mu), \tag{9}$$

from which (7) follows as a necessary and sufficient condition for the lemma to hold. ■

With the help of this lemma, we have the necessary and sufficient conditions to get the optimal phase shift selections. However, at this point, we assumed that the optimum μ would be given. To make use of this mathematical conditioning on the globally optimum solution, we need an operational framework to find μ, similar to [14], [19]. While μ can be anywhere on the unit circle, given the channel realizations h_n for $n = 0, 1, \ldots, N$, we provide the following proposition to reduce the search space of μ to a finite size, as an extension to [19, Proposition 1]. Towards that end, we will define the following sequence of complex numbers with respect to each $n = 1, 2, \ldots, N$ as

$$s_{nk} = \exp\left(j\left(\alpha_n + \phi_k - \frac{\omega_{k\ominus 1}}{2}\right)\right), \tag{10}$$

for $k = 1, 2, \ldots, K$. Define, for any two points a and b on the unit circle C, $\text{arc}(a : b)$ to be the unit circular arc with a as the initial end and b as the terminal end in the

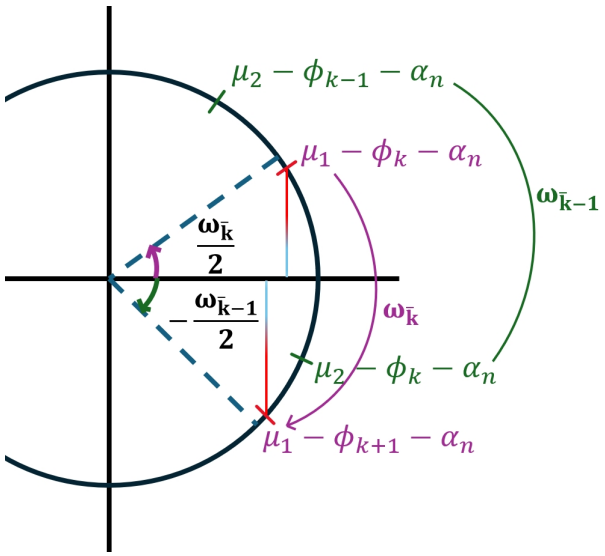

FIGURE 2: An illustration for the optimality of $\theta_n^* = \phi_k$ given $\mu \in \text{arc}(s_{nk} : s_{n,k+1})$.

counterclockwise direction, with the two endpoints a and b being excluded.

Proposition 1: A sufficient condition for $\theta_n^* = \phi_k$ is

$$\mu \in \text{arc}(s_{nk} : s_{n,k+1}). \tag{11}$$

Proof: Assume μ satisfies (11). Then,

$$\angle\underline{\mu} \in \left(\alpha_n + \phi_k - \frac{\omega_{k-1}}{2}, \alpha_n + \phi_{k+1} - \frac{\omega_k}{2}\right). \tag{12}$$

By subtracting θ_n and α_n, we get

$$\angle\underline{\mu} - \theta_n - \alpha_n \in \left(\phi_k - \frac{\omega_{k-1}}{2} - \theta_n, \phi_{k+1} - \frac{\omega_k}{2} - \theta_n\right). \tag{13}$$

Now, let $\theta_n = \phi_k$. Then,

$$\angle\underline{\mu} - \theta_n - \alpha_n \in \left(\phi_k - \frac{\omega_{k-1}}{2} - \phi_k, \phi_{k+1} - \frac{\omega_k}{2} - \phi_k\right). \tag{14}$$

By substituting $\phi_{k+1} = \phi_k + \omega_k$, we have

$$\angle\underline{\mu} - \theta_n - \alpha_n \in \left(-\frac{\omega_{k-1}}{2}, \frac{\omega_k}{2}\right). \tag{15}$$

Therefore, letting $\theta_n = \phi_k$ results in the largest $\cos(\theta_n + \alpha_n - \angle\underline{\mu})$ value among other possibilities for μ, as illustrated in Fig. 2 by showing the effect of selecting the phase shift option before and after than ϕ_k. Since $\cos(\angle\underline{\mu} - \theta_n - \alpha_n) = \cos(\theta_n + \alpha_n - \angle\underline{\mu})$, the proof is complete. ■

Finally, to operate with Proposition 1, we will eliminate duplicates among s_{nk} and sort to get $e^{j\lambda_l}$ such that $0 \leq \lambda_1 < \lambda_2 < \cdots < \lambda_L < 2\pi$. Define the update rule as

$$\mathcal{N}(\lambda_l) = \{\{n', k'\} | \angle s_{n'k'} = \lambda_l\}. \tag{16}$$

Let us search for the optimum μ by traversing the unit circle in the counterclockwise direction, starting from $\angle\underline{\mu} = 0$. With Proposition 1, we know that θ_n for $n = 1, 2, \ldots, N$ will remain the same unless μ switches from one arc to another. Whenever μ switches arcs, there exists n such that θ_n will be updated, i.e., if

$$\mu \in \text{arc}(e^{j\lambda_l} : e^{j\lambda_{l+1}}) \rightarrow \mu \in \text{arc}(e^{j\lambda_{l+1}} : e^{j\lambda_{l+2}}), \tag{17}$$

Algorithm 1 Generalized [19, Algorithm 1] for Nonuniform Phase Considerations

Initialization: Compute s_{nk} and $\mathcal{N}(\lambda_l)$ as in equations (10) and (16), respectively.
Set $\angle\underline{\mu} = 0$. For $n = 1, 2, \ldots, N$, calculate and store

$$\theta_n = \arg \max_{\theta_n \in \Phi_K} \cos(\angle\underline{\mu} - \theta_n - \alpha_n).$$

Set $g_0 = h_0 + \sum_{n=1}^{N} h_n e^{j\theta_n}$, $\texttt{absgmax} = |g_0|$.
for $l = 1, 2, \ldots, L-1$ **do**
  For each double $\{n', k'\} \in \mathcal{N}(\lambda_l)$, let $\theta_{n'} = \phi_{k'}$.
  Let

$$g_l = g_{l-1} + \sum_{\{n',k'\} \in \mathcal{N}(\lambda_l)} h_{n'}\left(e^{j\theta_{n'}} - e^{j(\phi_{k'} \ominus 1)}\right)$$

  if $|g_l| > \texttt{absgmax}$ **then**
    Let $\texttt{absgmax} = |g_l|$
    Store θ_n for $n = 1, 2, \ldots, N$
  end if
end for
Read out θ_n^* as the stored θ_n, $n = 1, 2, \ldots, N$.

then for every $\{n', k'\}$, $\theta_{n'}$ must be updated according to the update rule in (16) as

$$\theta_{n'} \rightarrow \phi_{k'}, \quad \{n', k'\} \in \mathcal{N}(\lambda_{l+1}). \tag{18}$$

Therefore, the optimum solution will come from $L \leq NK$ possible candidates of μ. For each candidate, we will operate using the sufficiency condition in Proposition 1 that is guaranteed to provide the globally optimum solution, since it is compatible with *Lemma 1*.

We specify the procedure explained in this section, which achieves the global optimum solution when RIS elements are strictly ON, as Algorithm 1. Algorithm 1 works as a search algorithm for the optimum μ and therefore the optimum RIS configuration, based on *Lemma 1* and *Proposition 1*. To initiate the search, Algorithm 1 starts with $\angle\underline{\mu} = 0$ and selects the RIS coefficients with *Lemma 1*. Then, to try every other candidate μ and the corresponding RIS configuration, Algorithm 1 only updates *one* or a small number of elements, as specified in (17) and (18), achieving linear time complexity. After trying NK or *fewer* options, Algorithm 1 selects the RIS configuration that achieves the maximum received power, which is guaranteed to be the global optimum by the analytical analysis provided in this section. A complexity analysis for Algorithm 1 is provided in Section X.

Finally, Algorithm 1 is a generalized version of [19, Algorithm 1] to work with nonuniform phase shifts and achieve the global optimum in $L \leq NK$ steps. We remark that, for uniformly distributed phase shifts, we showed in [19] that the convergence can be achieved in N or *fewer* steps, without requiring any complex number calculations.

Similar to what the authors in [20] pointed out, we remark on an important downside of the nonuniform discrete phase

shifts, especially when $R < \pi$. We know from our Proposition 1 that the optimal phase shift selections will satisfy $\underline{/\mu} - \theta_n - \alpha_n \in \left(-\frac{\omega_{k-1}}{2}, \frac{\omega_k}{2}\right)$. So, whenever $R < \pi$, we will have an $\omega_{\bar{k}} > \pi$ for $\bar{k} \in \{1, 2, \ldots, K\}$. Note that there could only be one instance of $\bar{k}$ since $\sum_{k=1}^{K} \omega_k = 2\pi$ must hold. With this, depending on the optimum μ, $\cos(\underline{/\mu} - \theta_n - \alpha_n)$ can take a negative value for some n. This results in a negative contribution to the optimum $|g|$ given in (9). To address the issue of negative values caused by $R < \pi$, we will discuss this in detail starting from Section VII and in subsequent sections.

IV. NONUNIFORM DISCRETE PHASE SHIFTS AND QUANTIZATION SOLUTION

In this section, we will approach the received power maximization problem with an intuitive quantization algorithm, which we call NPQ. This quantization approach is an extension to the uniform polar quantization (UPQ) algorithm proposed in [19]. It is similar to the closest point projection (CPP) algorithm in [12]. Using an analytical approach with this algorithm, we will develop closed-form solutions of the approximation ratios of arbitrary discrete phase shifts to the continuous solution, and develop a framework on how to place the nonuniform discrete phase shifts regarding the RIS phase range.

Consider the problem in (4) but without the condition $\theta_n \in \Phi_K$, $n = 1, 2, \ldots, N$. We call the solution of this problem the continuous solution to (4). Given a continuous solution to the problem in (4), say θ_n^{cont}, NPQ selects the closest possible angle from the set Φ_K. Therefore, for this purpose, we first relax θ_n and redefine the received power maximization problem as

$$\begin{aligned} &\underset{\boldsymbol{\theta}^{\text{cont}}}{\text{maximize}}\ f(\boldsymbol{\theta}^{\text{cont}}) \\ &\text{subject to } \theta_n^{\text{cont}} \in [-\pi, \pi),\ n = 1, 2, \ldots, N, \end{aligned} \tag{19}$$

where

$$f(\boldsymbol{\theta}^{\text{cont}}) = \left| \beta_0 e^{j\alpha_0} + \sum_{n=1}^{N} \beta_n e^{j(\alpha_n + \theta_n^{\text{cont}})} \right|^2. \tag{20}$$

In the above equation, $f(\boldsymbol{\theta}^{\text{cont}})$ is calculated by adding $N+1$ complex numbers, where each complex number represents a two-dimensional vector on the complex plane. Among $N+1$ vectors, the only vector we do not have control over is $h_0 = \beta_0 e^{j\alpha_0}$. Therefore, in order to achieve the maximum value of $f(\boldsymbol{\theta}^{\text{cont}})$, we can select

$$\theta_n^{\text{cont}} = \alpha_0 - \alpha_n,\ \text{for } n = 1, 2, \ldots, N, \tag{21}$$

so that all vectors will be aligned on top of each other, resulting in the maximum achievable value of $(\sum_{n=0}^{N} \beta_n)^2$. In other words,

$$\begin{aligned} f(\boldsymbol{\theta}^{\text{cont}}) &= |e^{j\alpha_0}|^2 \left| \beta_0 + \sum_{n=1}^{N} \beta_n e^{j(\alpha_n + \theta_n^{\text{cont}} - \alpha_0)} \right|^2 \\ &= \left| \beta_0 + \sum_{n=1}^{N} \beta_n e^{j(\alpha_n + \theta_n^{\text{cont}} - \alpha_0)} \right|^2 \end{aligned} \tag{22}$$

and the choice in (21) maximizes $f(\boldsymbol{\theta}^{\text{cont}})$. Given $\theta_n^{\text{cont}} \in [-\pi, \pi)$, NPQ projects to the closest available phase value in Φ_K. Therefore, assuming without loss of generality that $-\pi \le \phi_1 < \phi_2 < \cdots < \phi_K < \pi$, the decision rule for NPQ is defined as

$$\theta_n^{\text{NPQ}} = \begin{cases} \phi_1 & \text{if } -\pi \le \theta_n^{\text{cont}} < \dfrac{\phi_1 + \phi_2}{2}, \\ \phi_2 & \text{if } \dfrac{\phi_1 + \phi_2}{2} \le \theta_n^{\text{cont}} < \dfrac{\phi_2 + \phi_3}{2}, \\ \quad\vdots & \\ \phi_{K-1} & \text{if } \dfrac{\phi_{K-2} + \phi_{K-1}}{2} \le \theta_n^{\text{cont}} < \dfrac{\phi_{K-1} + \phi_K}{2}, \\ \phi_K & \text{otherwise.} \end{cases} \tag{23}$$

where θ_n^{cont} is the continuous solution in (21).

From the definition of NPQ, similar to UPQ and CPP approaches, the solution cannot be guaranteed to be globally optimum. In other words, NPQ can only provide a suboptimal solution. Yet, with the quantization approach, the beamforming process can be substantially simplified by using look-up tables, as NPQ only requires α_n for $n = 0, 1, \ldots, N$ to select the discrete phase shifts.

We present the cumulative distribution function (CDF) results for signal-to-noise ratio (SNR) Boost [14] in Fig. 3 for $K = 4$, and in Fig. 4 for $K = 8$. In these results, we consider the RIS phase range to be larger than or equal to π, i.e., $R \in \{180°, 240°\}$, leading us to use large values of K so that $R < 2\pi\frac{K-1}{K}$. The CDF results are presented for $N = 9$, 25, and 64, using 10,000 realizations of the channel model defined in [19] with $\kappa = 0$. We employed UPQ in [19] and the optimum algorithm [19, Algorithm 1] to generate the performance results for uniform discrete phase shifts and quantify the loss due to nonuniformity. We also employ Algorithm 1, and the NPQ algorithm presented in this paper, with the equally separated nonuniform discrete phase shifts structure given in Fig. 1. Finally, to provide a comparison with the literature, we employed the block coordinate descent (BCD) algorithm [24] as it is a commonly used approach [12], [14], [19], where phases are selected for each element at a time to successively refine the performance. All algorithms ran over the same channel realization in each step. Between Fig. 3 and Fig. 4, it can be seen that the loss due to the RIS phase range restriction increases for larger K. Note the UPQ with the uniform discrete phase shifts is always superior to NPQ, provided $R < 2\pi\frac{K-1}{K}$. However, we remark that the optimum performance provided by Algorithm 1 with nonuniform discrete phase shifts can surpass the UPQ algorithm with uniform phases. In other words, the loss due to the RIS phase range limitation is larger for the quantization approach rather than the optimum solution with $R \ge \pi$ and $\beta_n^r = 1$ for $n = 1, \ldots, N$.

In the next section, we will analyze the achievable performance under nonuniform discrete phase shift constraints by deriving approximation ratios with NPQ.

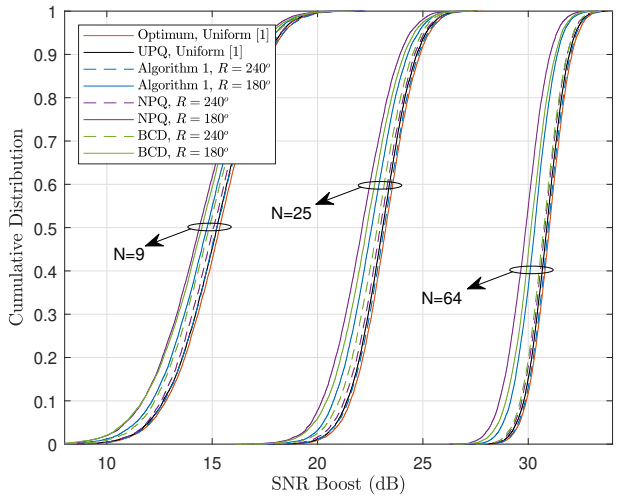

FIGURE 3: CDF plots for SNR Boost with [19, UPQ], [19, Algorithm 1], BCD [24], Algorithm 1, and NPQ, for $K = 4$.

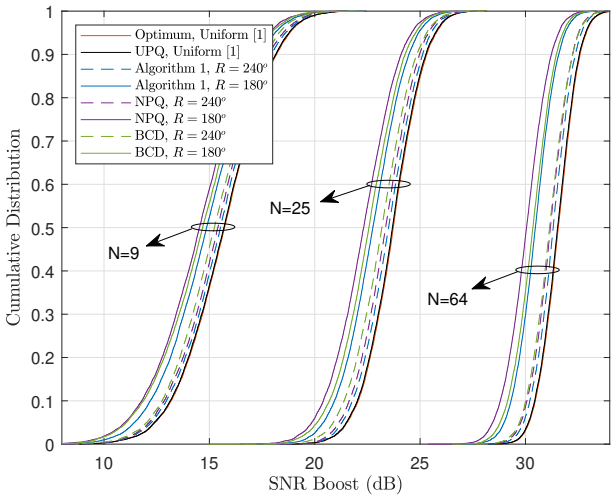

FIGURE 4: CDF plots for SNR Boost with [19, UPQ], [19, Algorithm 1], BCD [24], Algorithm 1, and NPQ, for $K = 8$.

V. APPROXIMATION RATIO OF NONUNIFORM DISCRETE PHASE SHIFTS WITH NPQ

Having the quantization approach in hand, we will define an approximation ratio to quantify the effect of the NPQ algorithm, the nonuniform discrete phase shifts, and the RIS phase range on the overall performance of the system. Specifically, the approximation ratio will quantify how well the continuous solution can be approximated. Similar to the approach in [9], [19], where we developed an approximation ratio for the UPQ algorithm [19] with uniform discrete phase shifts, we will first approximate the received power $f(\boldsymbol{\theta}^{\text{cont}})$ for asymptotically large N as

$$\begin{aligned} f(\boldsymbol{\theta}^{\text{NPQ}}) &= \left|\beta_0 e^{j\alpha_0} + \sum_{n=1}^{N} \beta_n e^{j(\alpha_n + \theta_n^{\text{NPQ}})}\right|^2 \\ &= \left|e^{j\alpha_0}\right|^2 \left|\beta_0 + \sum_{n=1}^{N} \beta_n e^{j(\alpha_n + \theta_n^{\text{NPQ}} - \alpha_0)}\right|^2 \\ &= \left|\beta_0 + \sum_{n=1}^{N} \beta_n e^{j(\theta_n^{\text{NPQ}} - \theta_n^{\text{cont}})}\right|^2 \\ &\approx \left|\sum_{n=1}^{N} \beta_n e^{j(\theta_n^{\text{NPQ}} - \theta_n^{\text{cont}})}\right|^2, \end{aligned} \tag{24}$$

where the gain from the direct link, i.e., β_0, is practically discarded. Let $\delta_n = \theta_n^{\text{NPQ}} - \theta_n^{\text{cont}}$ for $n = 1, 2, \ldots, N$. The resulting absolute square term in (24) can be expressed as

$$\begin{aligned} f(\boldsymbol{\theta}^{\text{NPQ}}) &\approx \left|\sum_{n=1}^{N} \beta_n e^{j(\theta_n^{\text{NPQ}} - \theta_n^{\text{cont}})}\right|^2 \\ &= \sum_{n=1}^{N} \beta_n^2 + 2\sum_{k=2}^{N}\sum_{l=1}^{k-1} \beta_k \beta_l \cos(\delta_k - \delta_l). \end{aligned} \tag{25}$$

Assume that in (25) all $\beta_k, \beta_l, \delta_k$, and δ_l are independent from each other. Taking the expectation yields

$$\mathbb{E}[f(\boldsymbol{\theta}^{\text{NPQ}})] = N\mathbb{E}[\beta_n^2] + N(N-1)\mathbb{E}[\beta_k\beta_l]\mathbb{E}[\cos(\delta_k - \delta_l)]. \tag{26}$$

Finally, we need to normalize the result in (26) with the maximum achievable result to get a ratio from 0 to 1, where the continuous solution would achieve 1. We know from (21) that the maximum achievable number is $(\sum_{n=0}^{N} \beta_n)^2$. Therefore, $\mathbb{E}[(\sum_{n=0}^{N} \beta_n)^2] = N\mathbb{E}[\beta_n^2] + N(N-1)\mathbb{E}[\beta_k\beta_l]$. As a result, with (26) , the ratio of the two expected values can be calculated for asymptotically large N as

$$\lim_{N\to\infty} \frac{\mathbb{E}[f(\boldsymbol{\theta}^{\text{NPQ}})]}{\mathbb{E}[(\sum_{n=0}^{N} \beta_n)^2]} = \mathbb{E}[\cos(\delta_k - \delta_l)]. \tag{27}$$

Hence, $\mathbb{E}[\cos(\delta_k - \delta_l)]$ will be the approximation ratio for NPQ. As we have the independence assumption among δ_k and δ_l, $\mathbb{E}[\cos(\delta_k - \delta_l)]$ can be simplified further as

$$\begin{aligned} &\mathbb{E}\left[\cos\left(\delta_k - \delta_l\right)\right] \\ &\quad = \mathbb{E}\left[\cos\left(\delta_k\right)\cos\left(\delta_l\right) + \sin\left(\delta_k\right)\sin\left(\delta_l\right)\right] \\ &\quad = \mathbb{E}\left[\cos\left(\delta_k\right)\cos\left(\delta_l\right)\right] + \mathbb{E}\left[\sin\left(\delta_k\right)\sin\left(\delta_l\right)\right] \\ &\quad = \mathbb{E}\left[\cos\left(\delta_k\right)\right]\mathbb{E}\left[\cos\left(\delta_l\right)\right] + \mathbb{E}\left[\sin\left(\delta_k\right)\right]\mathbb{E}\left[\sin\left(\delta_l\right)\right] \\ &\quad = \left(\mathbb{E}\left[\cos\left(\delta_n\right)\right]\right)^2 + \left(\mathbb{E}\left[\sin\left(\delta_n\right)\right]\right)^2 \end{aligned} \tag{28}$$

for $n = 1, 2, \ldots, N$. Therefore, for a given discrete phase shift selection set Φ_K, the approximation ratio can be calculated with (28). We will calculate this for two different scenarios. First, we will provide the approximation ratio for arbitrary ϕ_k, $k = 1, 2, \ldots, K$, and then for equally separated nonuniform phase shifts over the RIS phase range, as given in Fig. 1. In between the two steps, we will also analyze the special connection between the two and show that the latter maximizes the potential of the RIS with nonuniform discrete phase shifts.

Given the set Φ_K of arbitrary discrete phase shifts, the approximation ratio will be denoted by $E(\phi_1, \phi_2, \ldots, \phi_K)$. This will be a measure to represent the average performance for an RIS. For this purpose, as a common assumption from the literature to define the quantization error [9], [12], [19], we will assume that θ_n^{cont} is uniformly distributed, i.e., $\theta_n^{\text{cont}} \sim \mathcal{U}[-\pi, \pi]$ to apply the law of total expectation.

Let $\Phi_K = \{\phi_1, \phi_2, \ldots, \phi_K\}$ be the set of arbitrarily selected nonuniform phase shifts. Assume without loss of generality that $-\pi \leq \phi_1 < \phi_2 < \cdots < \phi_K < \pi$. Let $\theta_n^{\text{cont}} \in [\phi_k, \phi_{k+1}]$ for $k = 1, \ldots, K$ with probability $\frac{\phi_{k+1}-\phi_k}{2\pi}$, in which case θ_n^{NPQ} will either be ϕ_k or ϕ_{k+1}. Note that $\delta_n = \theta_n^{\text{NPQ}} - \theta_n^{\text{cont}}$ will be uniformly distributed in $\left[-\frac{\phi_{k+1}-\phi_k}{2}, \frac{\phi_{k+1}-\phi_k}{2}\right]$, i.e., $\delta_n \sim \mathcal{U}\left[-\frac{\phi_{k+1}-\phi_k}{2}, \frac{\phi_{k+1}-\phi_k}{2}\right]$.

To find $E(\phi_1, \phi_2, \ldots, \phi_K)$, we need to calculate the result in (28). First, note that the distribution of δ_n is always symmetric around zero, which gives $\left(\mathbb{E}\left[\sin\left(\delta_n\right)\right]\right)^2 = 0$, $n = 1, 2, \ldots, N$. Therefore, $E(\phi_1, \phi_2, \ldots, \phi_K) = \left(\mathbb{E}\left[\cos\left(\delta_n\right)\right]\right)^2$. Now, introduce the law of total expectation given as $\mathbb{E}[X] = \mathbb{E}[\mathbb{E}[X|Y]] = \sum_i \mathbb{E}[X|A_i]P(A_i)$, so that $\mathbb{E}\left[\cos\left(\delta_n\right)\right]$ can be calculated as

$$\begin{aligned}&\mathbb{E}\left[\cos\left(\delta_n\right)\right] = \\ &\sum_{k=1}^{K-1}\left[\frac{\phi_{k+1}-\phi_k}{2\pi}\int_{-\left(\frac{\phi_{k+1}-\phi_k}{2}\right)}^{\left(\frac{\phi_{k+1}-\phi_k}{2}\right)}\frac{1}{\phi_{k+1}-\phi_k}\cos(\delta_n)d\delta_n\right] \\ &+\frac{2\pi+\phi_1-\phi_K}{2\pi}\int_{-\left(\frac{2\pi+\phi_1-\phi_K}{2}\right)}^{\left(\frac{2\pi+\phi_1-\phi_K}{2}\right)}\frac{1}{2\pi+\phi_1-\phi_K}\cos(\delta_n)d\delta_n\end{aligned} \tag{29}$$

where inside the integral, $\frac{1}{\phi_{k+1}-\phi_k}$ comes from the uniform distribution and $\frac{\phi_{k+1}-\phi_k}{2\pi}$ is the probability of the event $\theta_n^{\text{cont}} \in [\phi_k, \phi_{k+1}]$ occurring. Now, we calculate the term inside the square brackets as

$$\begin{aligned}&\frac{\phi_{k+1}-\phi_k}{2\pi}\int_{-\left(\frac{\phi_{k+1}-\phi_k}{2}\right)}^{\left(\frac{\phi_{k+1}-\phi_k}{2}\right)}\frac{1}{\phi_{k+1}-\phi_k}\cos(\delta_n)d\delta_n \\ &\quad=\frac{1}{\pi}\int_0^{\left(\frac{\phi_{k+1}-\phi_k}{2}\right)}\cos(\delta_n)d\delta_n \\ &\quad=\frac{1}{\pi}\sin\left(\frac{\phi_{k+1}-\phi_k}{2}\right).\end{aligned} \tag{30}$$

Similarly, the last term in (29) will be $\frac{1}{\pi}\sin(\frac{\phi_K-\phi_1}{2})$ as $\sin(\frac{2\pi+\phi_1-\phi_K}{2}) = \sin(\frac{\phi_K-\phi_1}{2})$. Therefore, from equations (28), (29), and (30), the approximation ratio for an arbitrary nonuniform discrete phase shift set is

$$E(\boldsymbol{\phi}) = \frac{1}{\pi^2}\left[\left(\sum_{k=1}^{K-1}\sin\left(\frac{\phi_{k+1}-\phi_k}{2}\right)\right)+\sin\left(\frac{\phi_K-\phi_1}{2}\right)\right]^2 \tag{31}$$

where we used the shorthand notation $\boldsymbol{\phi}$ for $\phi_1, \phi_2, \ldots, \phi_K$ with $-\pi \leq \phi_1 < \phi_2 < \cdots < \phi_K < \pi$.

Now, without loss of generality, let $-\pi \leq \phi_1 < \cdots < \phi_K = \phi_1 + R < \pi$ with $R < 2\pi\frac{K-1}{K}$, as given in Fig. 1. Substituting $\phi_K = \phi_1 + R$ in (31), we have

$$\begin{aligned}E(\boldsymbol{\phi}) = \frac{1}{\pi^2}\Bigg[&\left(\sum_{k=1}^{K-2}\sin\left(\frac{\phi_{k+1}-\phi_k}{2}\right)\right) \\ &+\sin\left(\frac{\phi_1+R-\phi_{K-1}}{2}\right)+\sin\left(\frac{R}{2}\right)\Bigg]^2,\end{aligned} \tag{32}$$

where it is clear that R will directly impact the average performance. We leave the discussion of this to Section VI.

VI. OPTIMUM PLACEMENT OF THE PHASE SHIFTS

In this section, we use our approximation ratios calculated in Section V to find the optimal placement of the discrete phase shifts, analytically. More specifically, we first use equation (31) to show that the optimal placement of the discrete phase shifts would be uniformly distributed, when there is no RIS phase range limitation. Secondly, we extend this calculation considering a limited RIS phase range, i.e., $R < 2\pi\frac{K-1}{K}$, and show that the optimal placement of the discrete phase shifts would be equally separated over the RIS phase range, i.e., over $[-\frac{R}{2}\frac{R}{2}]$ as in Fig. 1. Finally, by considering the equally separated nonuniform discrete phase shifts, we reveal the effect of R and K on the overall discrete beamforming performance of the RIS. In (31), we derived the closed-form expression for the approximation ratio of the set of arbitrary nonuniform discrete phase shifts, i.e., how well the continuous solution can be approximated for large N. Now we will prove that given K, arranging the phase shifts uniformly will maximize the approximation ratio, and therefore will also maximize the average quantization performance. Define $\Delta_k = (\phi_{k+1} - \phi_k)/2$ for $k = 1, 2, \ldots, K-1$ and $\Delta_K = (2\pi + \phi_1 - \phi_K)/2$. Note that $\Delta_k \in (0, \pi)$ for $k = 1, 2, \ldots, K$ and $\sum_{k=1}^{K}\Delta_k = \pi$. Ignoring the factor $1/\pi^2$ in (31), the maximization problem can be equivalently expressed as

$$\begin{aligned}&\text{maximize } \sum_{k=1}^{K}\sin(\Delta_k) \\ &\text{subject to } \Delta_1+\Delta_2+\cdots+\Delta_K = \pi, \\ &\qquad\Delta_k \in (0,\pi),\ k = 1, 2, \ldots, K.\end{aligned} \tag{33}$$

Using Lagrange multipliers, let

$$\begin{aligned}&F(\Delta_1, \Delta_2, \ldots, \Delta_K, \lambda) \\ &\qquad=\sum_{k=1}^{K}\sin(\Delta_k)+\lambda\left(\sum_{k=1}^{K}\Delta_k-\pi\right),\end{aligned} \tag{34}$$

where, the derivatives will be

$$\begin{aligned}\frac{\partial F}{\partial \Delta_k} &= \cos(\Delta_k)+\lambda \\ \frac{\partial F}{\partial \lambda} &= \Delta_1+\Delta_2+\cdots+\Delta_K-\pi\end{aligned}$$

for $k = 1, 2, \ldots, K$. Letting $\frac{\partial F}{\partial \Delta_k} = 0$ gives $\cos(\Delta_1) = \cos(\Delta_2) = \cdots = \cos(\Delta_K) = -\lambda$. Since, $\Delta_k \in (0, \pi)$, the solution will be $\Delta_1 = \Delta_2 = \cdots = \Delta_K = \pi/K$ to satisfy the second condition $\frac{\partial F}{\partial \lambda} = 0$. Therefore, the optimum placement

of the phase shifts is uniformly distributed. Note that this is achievable as long as the RIS phase range R is large enough for a desired number of phase shifts K. Therefore, if there is to be a restriction due to the RIS phase range to force nonuniform phase shifts, the condition $R < 2\pi\frac{K-1}{K}$ must be satisfied. When there is a sufficient restriction due to the RIS, i.e., $R < 2\pi\frac{K-1}{K}$, there is no way that the arbitrary discrete phase shifts can be distributed uniformly over the range $[-\pi, \pi)$. However, we can still question the placement of the discrete phase shifts over the range R that the RIS can reach and show that equally separated discrete phase shifts over the range R will maximize the performance. Note from (32) that this time we need to define $\Delta_{k'}$ for $k' = 1, \ldots, K-1$. Therefore, let $\Delta_{k'} = \frac{\phi_{k'+1}-\phi_{k'}}{2}$, $k' = 1, \ldots, K-2$ and $\Delta_{K-1} = \frac{\phi_1+R-\phi_{K-1}}{2}$. Now, focusing on the placement of discrete phase shifts, we will omit the $\sin\left(\frac{R}{2}\right)$ term.

Similar to the arbitrary case, using the Lagrange multipliers, we define the equivalent maximization problem as

$$\begin{aligned} &\text{maximize} \sum_{k'=1}^{K-1} \sin(\Delta_{k'}) \\ &\text{subject to } \Delta_1 + \Delta_2 + \cdots + \Delta_{K-1} = \frac{R}{2}, \\ &\qquad \Delta_{k'} \in \left(0, \frac{R}{2}\right), \ k' = 1, 2, \ldots, K-1. \end{aligned} \tag{35}$$

Define

$$\begin{aligned} &F'(\Delta_1, \Delta_2, \ldots, \Delta_{K-1}, \lambda) = \\ &\qquad \sum_{k'=1}^{K-1} \sin(\Delta_{k'}) + \lambda \left(\sum_{k'=1}^{K-1} \Delta_{k'} - \frac{R}{2} \right), \end{aligned} \tag{36}$$

where, the derivatives will be

$$\begin{aligned} \frac{\partial F}{\partial \Delta_{k'}} &= \cos(\Delta_{k'}) + \lambda \\ \frac{\partial F}{\partial \lambda} &= \Delta_1 + \Delta_2 + \cdots + \Delta_{K-1} - \frac{R}{2} \end{aligned}$$

for $k' = 1, \ldots, K-1$. Letting $\frac{\partial F}{\partial \Delta_{k'}} = 0$ gives $\cos(\Delta_1) = \cos(\Delta_2) = \cdots = \cos(\Delta_{K-1}) = -\lambda$. Since $\Delta_{k'} \in (0, \frac{R}{2})$ and in this range the cosine function is monotonically decreasing, the solution is provided by $\Delta_1 = \Delta_2 = \cdots = \Delta_{K-1} = \frac{R}{2(K-1)}$. Note that this also satisfies $\frac{\partial F}{\partial \lambda} = 0$. Therefore, the optimum placement of the phase shifts is equally separated over the range R to maximize the average normalized performance of the RIS. At this point, we have shown that given the RIS phase range R, the placement of the nonuniform discrete phase shifts over the RIS phase range needs to be equally separated, to harness the potential of the RIS and maximize the approximation ratio. This placement of the nonuniform phase shifts will also be adopted for the rest of the paper, including the numerical results, as suggested by the performance maximization approach and practicality. Therefore, as shown in Fig. 1, we let $\Phi_K = \left\{-\frac{R}{2}, \frac{R}{K-1} - \frac{R}{2}, 2\frac{R}{K-1} - \frac{R}{2}, \ldots, \ (K-1)\frac{R}{K-1} - \frac{R}{2}\right\}$. So that, with the equally separated discrete phase shifts, the

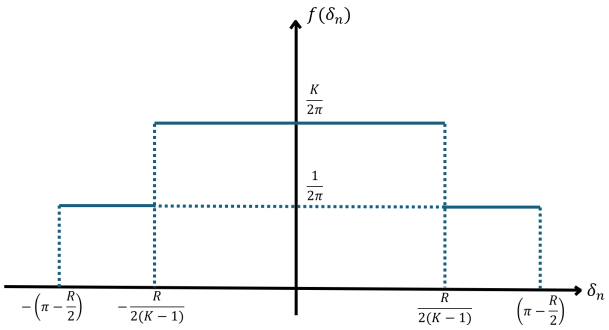

FIGURE 5: PDF of δ_n, i.e., the quantization error.

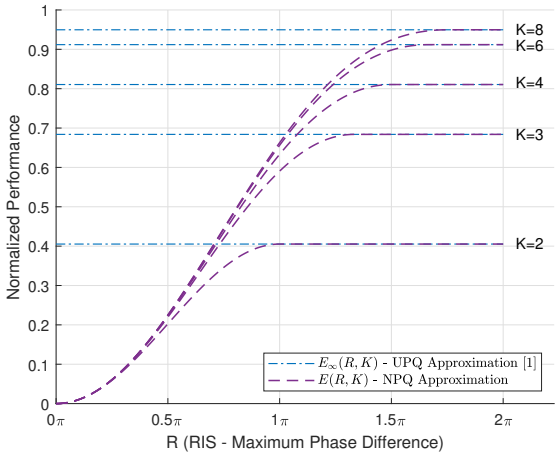

FIGURE 6: $E(R, K)$ vs R for $K \in \{2, 3, 4, 6, 8\}$

decision rule for the NPQ can alternatively be defined as

$$\theta_n^{\text{NPQ}} = \begin{cases} \frac{R}{2} & \text{if} \quad \frac{R}{2} \leq \theta_n^{\text{cont}}, \\ \left\lfloor \frac{\theta_n^{\text{cont}} + \frac{R}{2}}{\omega'} \right\rceil \times \omega' - \frac{R}{2} & \text{if} \quad -\frac{R}{2} \leq \theta_n^{\text{cont}} < \frac{R}{2}, \\ -\frac{R}{2} & \text{if} \quad \theta_n^{\text{cont}} < -\frac{R}{2}, \end{cases} \tag{37}$$

where $\lfloor \cdot \rceil$ is the rounding function defined as $\lfloor x \rceil = \text{sgn}(x) \lfloor |x| + 0.5 \rfloor$ and $\omega' = \frac{R}{K-1}$.

Let us define the approximation ratio as $E(R, K) = \mathbb{E}[\cos(\delta_k - \delta_l)]$, where we have $\delta_n = \theta_n^{\text{NPQ}} - \theta_n^{\text{cont}}$. From the definition of θ_n^{NPQ} and θ_n^{cont} in (37) and (21) respectively, clearly $\delta_n \in \left[-(\pi - \frac{R}{2}), \pi - \frac{R}{2}\right]$. Remembering the assumption that $\theta_n^{\text{cont}} \sim \mathcal{U}[-\pi, \pi]$, the probability density function (PDF) of δ_n, i.e., $f(\delta_n)$, can be deduced simply and it is plotted in Fig. 5. With the PDF $f(\delta_n)$, we need to calculate the simplified version of the term $\mathbb{E}[\cos(\delta_k - \delta_l)]$ as given in (28). Note that, the second term in (28) will be zero, since $f(\delta_n)$ is an even function. Therefore, we only need to calculate $\left(\mathbb{E}[\cos(\delta_n)]\right)^2$ to find $E(R, K)$. Let us first calculate $\mathbb{E}[\cos(\delta_n)]$ as

$$\mathbb{E}[\cos(\delta_n)]$$

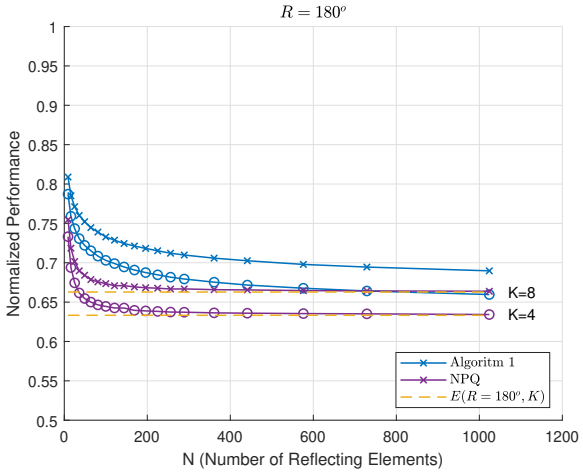

FIGURE 7: Normalized Performance results vs. N, for $R = 180°$ and $K \in \{4, 8\}$.

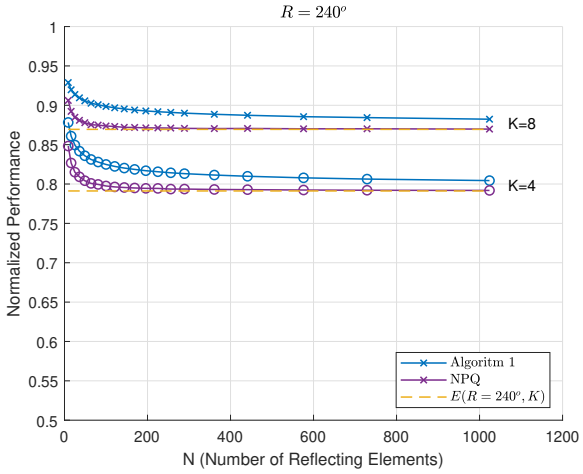

FIGURE 8: Normalized Performance results vs. N, for $R = 240°$ and $K \in \{4, 8\}$.

$$= 2\left[\int_0^{\frac{R}{2(K-1)}} \cos(\delta_n)\frac{K}{2\pi}\,d\delta_n + \int_{\frac{R}{2(K-1)}}^{\pi-R/2} \cos(\delta_n)\frac{1}{2\pi}\,d\delta_n\right]$$

$$= \frac{1}{\pi}\left[K\left[\sin\left(\frac{R}{2(K-1)}\right) - \sin(0)\right] + \left[\sin\left(\pi - \frac{R}{2}\right) - \sin\left(\frac{R}{2(K-1)}\right)\right]\right]$$

$$= \frac{1}{\pi}\left[(K-1)\sin\left(\frac{R}{2(K-1)}\right) + \sin\left(\frac{R}{2}\right)\right] \quad (38)$$

$$= \frac{R}{2\pi}\left[\text{sincu}\left(\frac{R}{2(K-1)}\right) + \text{sincu}\left(\frac{R}{2}\right)\right] \quad (39)$$

where from (38) to (39), we divide and multiply by $R/2$, and $\text{sincu}(\cdot)$ represents the unnormalized sinc function $\text{sincu}(x) = \frac{\sin x}{x}$. Note that $\text{sincu}(x) = \text{sinc}(\frac{x}{\pi})$. Also, note that (38) is compatible with (31) with $\frac{\phi_{k+1}-\phi_k}{2} = \frac{R}{2(K-1)}$ for $k = 1, \ldots, K-1$ and $\frac{\phi_K - \phi_1}{2} = \frac{R}{2}$. Thus, the approximation ratio for the NPQ algorithm is

$$E(R, K) = \frac{R^2}{4\pi^2}\left[\text{sinc}\left(\frac{R}{2\pi(K-1)}\right) + \text{sinc}\left(\frac{R}{2\pi}\right)\right]^2 \quad (40)$$

where R is the RIS phase range and $\text{sinc}(\cdot)$ is normalized satisfying $\text{sinc}(1) = 0$. An illustration for the theoretical calculations of the approximation $E(R, K)$ is given in Fig. 6, where it can be seen that $E(R, K)$ converges to the approximation ratio of the uniform phases, i.e., $E_\infty(K)$ in [19], as the RIS phase range increases. From our analysis of the optimum selection of nonuniform discrete phases in Section VI, we know that the equal separation in the RIS phase range will maximize the average performance. Even with the best case scenario with the optimal placement of the nonuniform phases, Fig. 6 shows that the gain of using $K \geq 3$ is only marginal when $R < \pi/2$. Similarly, the gain of using $K = 4$ or more discrete phase shifts is negligible unless the RIS phase range is large enough, i.e., $R > \pi$. We remark that the approximation ratio is calculated for sufficiently large N. Further analysis to confirm the validity of the theoretical calculation of $E(R, K)$ is provided in the numerical results.

Finally, the numerical results for the approximation ratio are calculated by dividing the expression $\left|\beta_0 e^{j\alpha_0} + \sum_{n=1}^{N} \beta_n e^{j(\alpha_n+\theta_n)}\right|^2$ to $(\sum_{n=0}^{N} \beta_n)^2$ for each channel realization and averaged. With this, the normalized performance results are presented in Fig. 7 for $R = 180°$, and in Fig. 8 for $R = 240°$. In both figures, the performance of NPQ converges to the approximation ratio curve for large N, falling in line with our analytical analysis on $E(R, K)$. Providing the optimum result, Algorithm 1 serves as an upper bound. From Fig. 7 to Fig. 8, for larger R, the performance gap between Algorithm 1 and NPQ gets smaller. With this, we remark that increasing R from $180°$ to $240°$ helps significantly more in terms of performance rather than increasing the number of discrete phase shifts K. This confirms our analysis with Fig. 6 that the lower the RIS phase range is, the less likely it is to achieve a performance gain by increasing K.

VII. GLOBAL OPTIMUM SOLUTION WITH ON/OFF β_n^r

In this section, we address the destructive selection issue by relaxing the RIS gains, i.e., $\beta_n^r \in [0, 1]$. With this, we will define an updated maximization problem where we tune β_n^r together with θ_n, and develop an optimal discrete phase shift selection algorithm with ON/OFF β_n^r. We will also specify how it can converge to the optimum solution in $L \leq N(K+1)$ steps in linear time.

So far, we have developed a comprehensive analysis for the approximation ratio of nonuniform discrete phase shifts. Together with this, we provided two algorithms, i.e., NPQ and Algorithm 1, where the first is an intuitive practical algorithm and the latter achieves the global optimum with $\beta_n^r = 1$ for $n = 1, 2, \ldots, N$ in NK or fewer steps, provided

$R \geq \pi$. Then, we underlined the special case that arises due to the nonuniform structure of the phase shifts, or the RIS phase range constraint, that setting $\beta_n^r = 1$ for $n = 1, 2, \ldots, N$ right away can result in allowing paths that are destructive when $R < \pi$.

In this section, we will develop a new algorithm, Algorithm 2, for the special case of $R < \pi$. We will also show that this algorithm can be interchangeably used with Algorithm 1 with relaxed β_n^r. Algorithm 2 will adjust the RIS gains to manage the destructive paths through the RIS. For this purpose, we will relax the gains and redefine the optimization problem as

$$\begin{aligned} &\underset{\boldsymbol{\theta}}{\text{maximize}}\ f(\boldsymbol{\theta}) \\ &\text{subject to } \theta_n \in \Phi_K,\ n = 1, 2, \ldots, N \\ &\qquad\qquad \beta_n^r \in [0, 1],\ n = 1, 2, \ldots, N \end{aligned} \tag{41}$$

where

$$f(\boldsymbol{\theta}) = \left| \beta_0 e^{j\alpha_0} + \sum_{n=1}^{N} \beta_n \beta_n^r e^{j(\alpha_n + \theta_n)} \right|^2, \tag{42}$$

$\beta_n > 0,\ n = 0, 1, \ldots, N$, $\boldsymbol{\theta} = (\theta_1, \theta_2, \ldots, \theta_N)$, and $\alpha_n \in [-\pi, \pi)$ for $n = 0, 1, \ldots, N$.

Similar to our *Lemma 1*, let

$$g' = h_0 + \sum_{n=1}^{N} h_n \beta_n^{r*} e^{j\theta_n^*}, \tag{43}$$

so that we can state our second lemma as follows.

Lemma 2: To achieve the maximum of $|g'|$, a necessary condition on $(\theta_1^*, \theta_2^*, \ldots, \theta_n^*)$ is that each θ_n^* for $n \in \{n | \beta_n^{r*} > 0\}$ must satisfy

$$\theta_n^* = \arg \max_{\theta_n \in \Phi_K} \cos(\theta_n + \alpha_n - \underline{\angle \mu}) \tag{44}$$

where $\underline{\angle \mu}$ stands for the phase of optimum $\mu = g'/|g'|$ with g' in equation (43).

Proof: We can rewrite equation (9) as

$$|g'| = \beta_0 \cos(\alpha_0 - \underline{\angle \mu}) + \sum_{n=1}^{N} \beta_n \beta_n^r \cos(\theta_n^* + \alpha_n - \underline{\angle \mu}), \tag{45}$$

where $\beta_n > 0$. Therefore, for $|g'|$ to be the maximum value possible, (44) follows as a necessary condition, completing the proof. ■

So far, similar to the development of Algorithm 1, we are proceeding with the assumption that we know the optimum μ. Before coming up with the operational procedure for Algorithm 2, we will state our third lemma regarding the optimum RIS gain selection β_n^{r*} as follows:

Lemma 3: Given the optimum μ, the globally optimum solution will be yielded by $\beta_n^{r*} = \lceil \cos(\theta_n^* + \alpha_n - \underline{\angle \mu}) \rceil$.

Proof: In equation (45), define the function $h(\beta_n^r) = \beta_n \beta_n^r \cos(\theta_n^* + \alpha_n - \underline{\angle \mu})$ independently for every $n = 1, 2, \ldots, N$. For $|g'|$ to be the maximum value possible, given θ_n^*, the function $h(\beta_n^r)$ should be maximized independently for $n = 1, \ldots, N$. Note that $h(\beta_n^r)$ is a monotonic function.

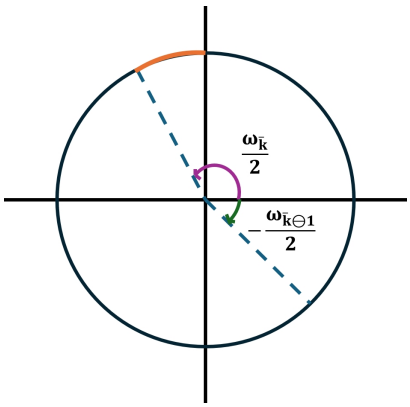

FIGURE 9: Range of values of $\angle\mu - \theta_n - \alpha_n$ for Case 1 with $\mu \in \text{arc}(s_{n\bar{k}} : s_{n,\bar{k}\oplus 1})$.

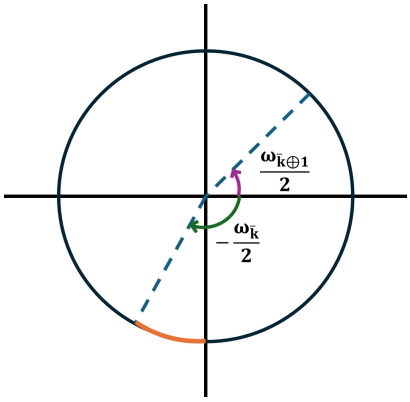

FIGURE 10: Range of values of $\angle\mu - \theta_n^* - \alpha_n$ for Case 2 with $\mu \in \text{arc}(s_{n,\bar{k}\oplus 1} : s_{n,\bar{k}\oplus 2})$.

Therefore, to achieve the maximization in $|g'|$, β_n^{r*} needs to satisfy

$$\beta_n^{r^*} = \begin{cases} 1, & \text{if } \cos(\theta_n^* + \alpha_n - \angle\mu) > 0, \\ 0, & \text{if } \cos(\theta_n^* + \alpha_n - \angle\mu) \leq 0. \end{cases} \tag{46}$$

Therefore, without loss of generality, the optimum solution will be yielded by ON/OFF β_n^r provided by the equality

$$\beta_n^r = \lceil \cos(\theta_n + \alpha_n - \underline{\angle \mu}) \rceil. \tag{47}$$

Therefore, the proof is complete. ■

To operate with *Lemma 3*, further analysis is required in terms of finding when the $\cos(\theta_n^* + \alpha_n - \angle\mu) < 0$ case will arise. For this purpose, assume for $R < \pi$ that we have the unique $\bar{k}$ such that $\omega_{\bar{k}} > \pi$. We will revisit equation (15) from Proposition 1, as we know from Lemma 2 that it will hold whenever $\beta_n^r > 0$. Our θ_n^* selections will make sure that $\underline{\angle \mu} - \theta_n - \alpha_n \in \left(-\frac{\omega_{k-1}}{2}, \frac{\omega_k}{2}\right)$, given that $\mu \in \text{arc}(s_{nk} : s_{n,k+1})$. Consider two cases, $\mu \in \text{arc}(s_{n\bar{k}} : s_{n,\bar{k}\oplus 1})$ and $\mu \in \text{arc}(s_{n,\bar{k}\oplus 1} : s_{n,\bar{k}\oplus 2})$. As shown in Fig. 9 and Fig. 10, in both cases the cosine value in (45) can take a negative value, i.e., $\cos(\theta_n + \alpha_n - \angle\mu) < 0$, resulting in the selection of $\beta_n^r = 0$. With this observation, we propose the following proposition to be able to operate with *Lemma 2* and *Lemma 3*.

Proposition 2: Let $s^1_{n,\bar{k}\oplus 1} = e^{j(\alpha_n+\phi_{\bar{k}}+\frac{\pi}{2})}$ and $s^2_{n,\bar{k}\oplus 1} = e^{j(\alpha_n+\phi_{\bar{k}\oplus 1}-\frac{\pi}{2})}$. A sufficient condition for $\beta_n^{r*} = 0$ is

$$\mu \in \text{arc}(s^1_{n,\bar{k}\oplus 1} : s^2_{n,\bar{k}\oplus 1}). \tag{48}$$

Proof: Consider the two and only cases that $\cos(\theta_n+\alpha_n-\angle\mu)$ can take a negative value.

First, assume $\mu \in \text{arc}(s_{n\bar{k}} : s_{n,\bar{k}\oplus 1})$. Since $\omega_{\bar{k}}/2 > \pi/2$, the cosine value can take a negative value as shown in Fig. 9. This happens if $\mu \in \text{arc}(s_{n,\bar{k}\oplus 1}e^{-j(\omega_{\bar{k}}-\pi)/2} : s_{n,\bar{k}\oplus 1})$, as there is no $\theta_n \in \Phi_K$ such that $\cos(\theta_n+\alpha_n-\angle\mu) > 0$.

Second, assume $\mu \in \text{arc}(s_{n,\bar{k}\oplus 1} : s_{n,\bar{k}\oplus 2})$. Since $-\omega_{\bar{k}}/2 < -\pi/2$, the cosine value can take a negative value as shown in Fig. 10. This happens if $\mu \in \text{arc}(s_{n,\bar{k}\oplus 1} : s_{n,\bar{k}\oplus 1}e^{j(\omega_{\bar{k}}-\pi)/2})$, as there is no $\theta_n \in \Phi_K$ such that $\cos(\theta_n+\alpha_n-\angle\mu) > 0$.

Finally, the two cases together can be expressed as a single arc around $s_{n,\bar{k}\oplus 1}$ by using $s^1_{n,\bar{k}\oplus 1}$ and $s^2_{n,\bar{k}\oplus 1}$ as $\mu \in \text{arc}(s_{n,\bar{k}\oplus 1}e^{-j(\omega_{\bar{k}}-\pi)/2} : s_{n,\bar{k}\oplus 1}e^{j(\omega_{\bar{k}}-\pi)/2})$. Since $\phi_{\bar{k}\oplus 1} = \phi_{\bar{k}} + \omega_{\bar{k}}$, the same arc can be expressed as $\mu \in \text{arc}(e^{j(\alpha_n+\phi_{\bar{k}}+\frac{\pi}{2})} : e^{j(\alpha_n+\phi_{\bar{k}\oplus 1}-\frac{\pi}{2})})$. Thus, the proof is complete. ■

With Proposition 1 and Proposition 2 together, we need to consider $K+1$ arcs that the optimum μ can be in for every $n = 1, \ldots, N$ independently as there is an extra arc introduced in Proposition 2 for $n = 1, 2, \ldots, N$. This is because, when $R < \pi$ and $\omega_{\bar{k}} > \pi$, we will let $s_{n,\bar{k}\oplus 1} = \{s^1_{n,\bar{k}\oplus 1}, s^2_{n,\bar{k}\oplus 1}\}$ so that $s_{n,\bar{k}\oplus 1}$ will encode two complex numbers.

We specify the procedure explained in this section, which achieves the global optimum solution when the RIS gains are relaxed, i.e., $\beta_n^r \in [0, 1]$, as Algorithm 2. Like Algorithm 1, Algorithm 2 works as a search algorithm for the optimum μ and therefore the optimum RIS configuration, based on *Lemma 2*, *Lemma 3*, and *Proposition 2*. To initiate the search, Algorithm 2 starts with $\underline{/\mu} = 0$ and selects the RIS coefficients with *Lemma 2* and *Lemma 3*. Then, to try every other candidate μ and the corresponding RIS configuration, Algorithm 2 only updates *one* or a small number of elements, e.g., it may turn ON/OFF or update the phase of these elements, achieving linear time complexity. After trying $N(K+1)$ or *fewer* options, Algorithm 2 selects the RIS configuration that achieves the maximum received power that is guaranteed to be the global optimum by the analytical analysis provided in this section. A complexity analysis for Algorithm 2 is provided in Section X. We remark that Algorithm 2 works with adjustable RIS gains, yet it achieves the global optimum solution by setting an element either ON or OFF. Also, note that Algorithm 2 is an extended version of Algorithm 1 in Section III to work with adjustable RIS gains when $R < \pi$.

We present the CDF results for SNR Boost in Fig. 11 for $K = 2$, and in Fig. 12 for $K = 4$. In these results, we consider a notable limitation on the RIS phase range such that $R < \pi$, i.e., $R \in \{90^\circ, 120^\circ\}$. The CDF results are presented for $N = 16$, 64, and 256, using 10,000 realizations of the channel model defined in [19] with $\kappa = 0$. The discrete phase shift selections are equally separated and chosen as given in Fig. 1. We employed Algorithm 1, Algorithm 2, and NPQ algorithms that we proposed in this paper, as well as BCD algorithm [24]. Since we have $R < \pi$, Algorithm 1 will only serve as a pseudo-optimal solution, assuming that β_n^r are strictly 1 for all n, so that we can observe the effect of destructive paths and ON/OFF keying. All algorithms ran over the same channel realization in each step. It can be seen that the gap between Algorithm 2 and the other algorithms increases for larger N, as well as for smaller R. This signifies the power of using ON/OFF β_n^r with larger RISs, having more phase range limitations. Furthermore, using $K = 4$

Algorithm 2 Extended Algorithm 1 for the Special Condition When $R < \pi$.

Initialization: Compute s_{nk} and $\mathcal{N}(\lambda_l)$ as in Proposition 2 and equation (16), respectively.
Set $\underline{/\mu} = 0$. For $n = 1, 2, \ldots, N$, calculate

$$\theta_n = \arg\max_{\theta_n \in \Phi_K} \cos(\underline{/\mu} - \theta_n - \alpha_n).$$

Set $\beta_n^r = \lceil \cos(\underline{/\mu} - \theta_n - \alpha_n) \rceil$ for $n = 1, 2, \ldots, N$.
Update $\theta_n = \phi_{\bar{k}\oplus 1}$ for $n \in \{n | \beta_n^r = 0\}$, and store $\theta_n, \forall n$.
Set $g_0 = h_0 + \sum_{n=1}^N h_n \beta_n^r e^{j\theta_n}$, $\texttt{absgmax} = |g_0|$.
for $l = 1, 2, \ldots, L'-1$ **do**
  Set $g_{\texttt{update}} = 0$.
  for each double $\{n', k'\} \in \mathcal{N}(\lambda_l)$ **do**
    if $\beta_{n'} = 1$ **then**
      if $k' = \bar{k} \oplus 1$ **then**
        Set $\beta_{n'} = 0$ and $\theta_{n'} = \phi_{k'}$
        Let

$$g_{\texttt{update}} - h_{n'} e^{j\phi_{\bar{k}}} \leftarrow g_{\texttt{update}}.$$

      else
        Set $\theta_{n'} = \phi_{k'}$
        Let

$$g_{\texttt{update}} + h_{n'}\left(e^{j\theta_{n'}} - e^{j(\phi_{k'}\ominus 1)}\right) \leftarrow g_{\texttt{update}}.$$

      end if
    else
      Set $\beta_{n'} = 1$
      Let

$$g_{\texttt{update}} + h_{n'} e^{j\theta_{n'}} \leftarrow g_{\texttt{update}}.$$

    end if
  end for
  Let $g_l = g_{l-1} + g_{\texttt{update}}$
  if $|g_l| > \texttt{absgmax}$ **then**
    Let $\texttt{absgmax} = |g_l|$
    Store β_n^r and θ_n for $n = 1, 2, \ldots, N$
  end if
end for
Read out $\beta_n^{r^*}$ and θ_n^*, $n = 1, 2, \ldots, N$.

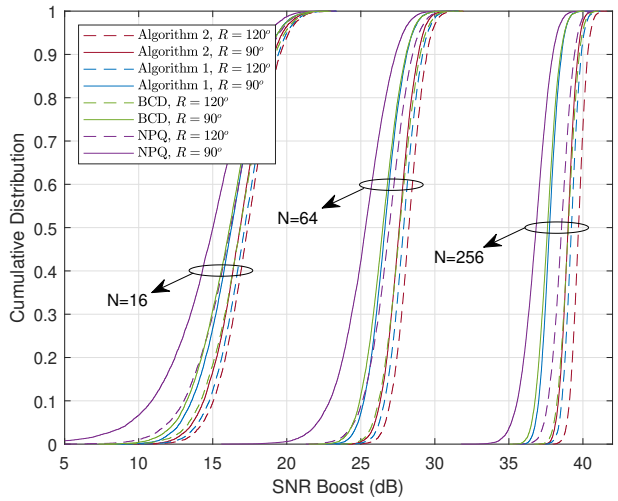

FIGURE 11: CDF plots for SNR Boost with BCD [24], nonuniform polar quantization (NPQ), Algorithm 1, and Algorithm 2 for $K = 2$ and $R \in \{90°, 120°\}$.

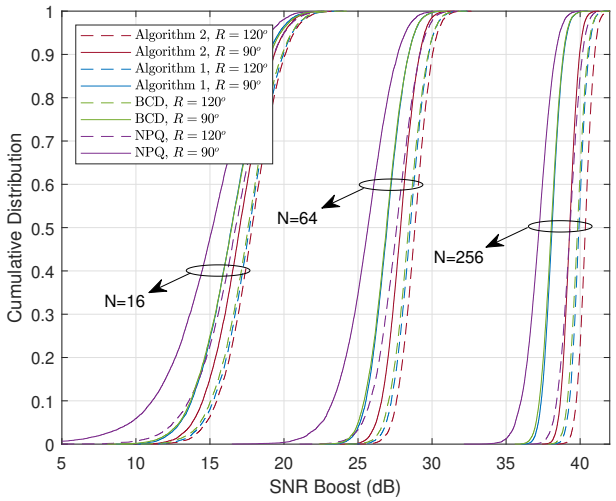

FIGURE 12: CDF plots for SNR Boost with BCD [24], nonuniform polar quantization (NPQ), Algorithm 1, and Algorithm 2 for $K = 4$ and $R \in \{90°, 120°\}$.

instead of $K = 2$ mostly impacts the performance of NPQ with $R = 120°$, making it more desirable due to its low complexity. Finally, BCD can outperform NPQ, as it is seemingly benefiting from the phase range restriction, e.g., this can be observed by comparing Fig. 3 and Fig. 12. Yet, BCD is still outperformed by Algorithm 1.

With Algorithm 2 and $R < \pi$, the normalized performance results are presented in Fig. 13 for $R = 90°$, and in Fig. 14 for $R = 120°$. In both figures, the performance of NPQ converges to the approximation ratio curve for large N, again confirming our analytical analysis on $E(R, K)$. Similar to the CDF plots, the performance gain from using Algorithm 2 over both NPQ and Algorithm 1 increases for larger N. Also, if R is sufficiently low, Algorithm 2 is always superior to Algorithm 1. Similarly, Algorithm 1 is always superior to NPQ, even if a larger K is used for the latter. The underlying reason for this again is that the performance gain from using larger K diminishes significantly for low R.

Finally, we present the average SNR Boost results of our proposed algorithms versus R in Fig. 15 for $K = 2$, and in Fig. 16 for $K = 4$. Both figures show that the average performance of Algorithm 1 converges to that of Algorithm 2, as R approaches π. On the other hand, NPQ can provide an average SNR Boost that is significantly close to both Algorithm 1 and Algorithm 2 as R increases, for large N. Both Fig. 15 and Fig. 16 suggest in a sense that Algorithm 1 and Algorithm 2 can be used interchangeably to solve the problem in (41), where the selection depends on whether $R < \pi$ or $R \geq \pi$.

Finally, we remark that the development of Algorithm 2 follows from the strict limitation on the RIS phase range, i.e., $R < \pi$. Otherwise, an important side conclusion that follows from *Lemma 3* is that, Algorithm 1 can be extended to solve the problem in (41) with $\beta_n^r \in [0, 1]$ for $n = 1, 2, \ldots, N$, when $R > \pi$. With $R > \pi$, we know from *Lemma 3* that the solution that yields the global optimum will select $\beta_n^r = 1$ for $n = 1, 2, \ldots, N$. Therefore, both Algorithm 1 and Algorithm 2 can be used to solve the general problem in (41) for $R \geq \pi$ and $R < \pi$, respectively. With this, the number of required steps in the **for** loop would reduce from $N(K+1)$ to NK. Further analysis regarding the number of required steps and complexity is provided in the following section.

VIII. REVISITING THE QUANTIZATION SOLUTION WITH ON/OFF β_n^r: EXTENDED NONUNIFORM POLAR QUANTIZATION

In this section, we will propose a novel quantization algorithm by enhancing the NPQ algorithm with ON/OFF β_n^r selections. The importance of the ON/OFF selections has been established so far, showing significant performance gains for $R < \pi$. A similar approach to exploit β_n^r in Algorithm 2 can be used for the quantization solution.

The quantization approach comes from selecting the closest option from the phase shifts set to the continuous solution, which can achieve the maximum possible received power given by $(\sum_{n=0}^{N} \beta_n)^2$. Similar to our analysis in Section VII, let $\delta_n = \theta_n^{\text{NPQ}} - \theta_n^{\text{cont}}$ for $n = 1, \ldots, N$. When $R < \pi$, depending on the value θ_n^{cont}, the difference between θ_n^{NPQ} and θ_n^{cont} in (21) can be greater than $\frac{\pi}{2}$, or less than $-\frac{\pi}{2}$, i.e., $|\delta_n| > \frac{\pi}{2}$. Therefore, such a path through the nth RIS element would contribute destructively to the overall performance, as could be deduced from $E(R, K) = (\mathbb{E}[\cos(\delta_n)])^2$. With the adjustable RIS gains, this can be eliminated by an OFF selection, i.e., $\beta_n^r = 0$. Therefore, we define the ENPQ algorithm with ON/OFF β_n^r, which is an algorithm to select

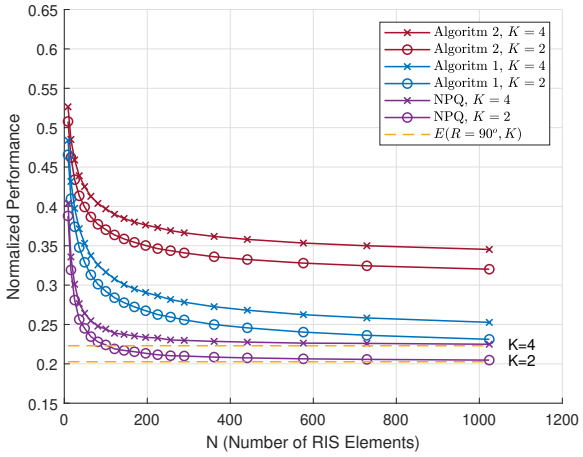

FIGURE 13: Normalized Performance results vs. N, for $R = 90°$ and $K \in \{2, 4\}$.

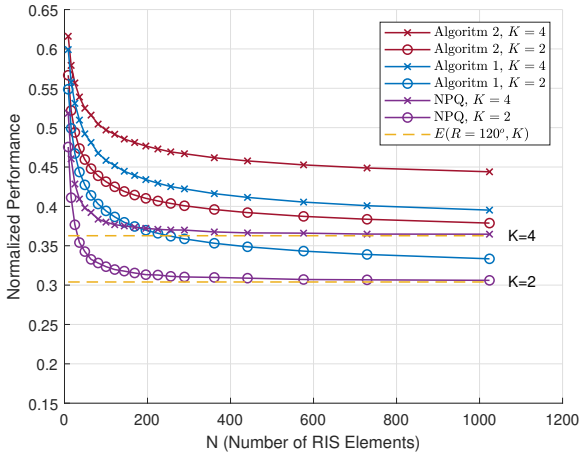

FIGURE 14: Normalized Performance results vs. N, for $R = 120°$ and $K \in \{2, 4\}$.

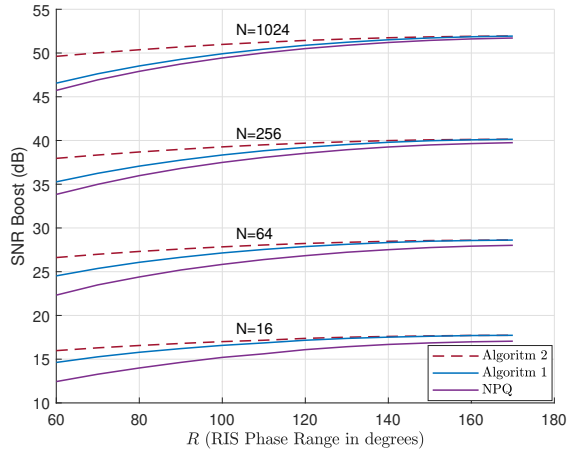

FIGURE 15: Average SNR Boost vs. R, for $K = 2$ and $N \in \{16, 64, 256, 1024\}$.

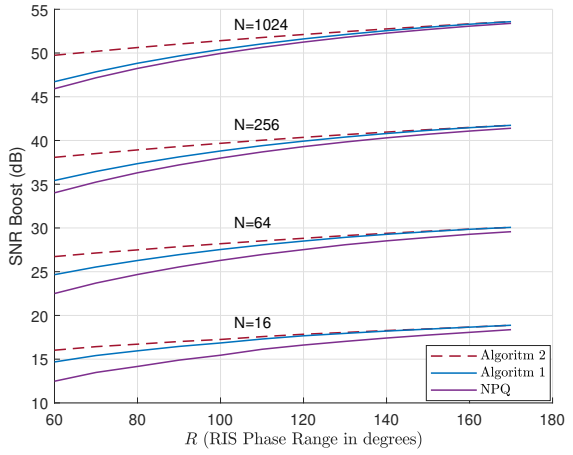

FIGURE 16: Average SNR Boost vs. R, for $K = 4$ and $N \in \{16, 64, 256, 1024\}$.

the RIS coefficients, as

$$\mathrm{w}_n^{\mathrm{ENPQ}} = \lceil \cos(\delta_n) \rceil \exp\left(j\theta_n^{\mathrm{NPQ}}\right), \tag{49}$$

where θ_n^{NPQ} are selected by the NPQ algorithm, and $\delta_n = \theta_n^{\mathrm{NPQ}} - \theta_n^{\mathrm{cont}}$. Note that for $R \geq \pi$, ENPQ will select the same RIS coefficients as the NPQ algorithm, because $|\delta_n| > \frac{\pi}{2}$ will never occur.

IX. APPROXIMATION RATIO CALCULATION FOR ENPQ

We extend our approximation ratio calculations to find the approximation ratio for the ENPQ algorithm, i.e., $E_{\mathrm{off}}^{\mathrm{on}}(R, K)$. With the independence assumption among δ_n, it can be deduced from (25)–(28) that $E_{\mathrm{off}}^{\mathrm{on}}(R, K) = \left(\mathbb{E}\left[\lceil \cos(\delta_n) \rceil \cos\left(\delta_n\right)\right]\right)^2 + \left(\mathbb{E}\left[\lceil \cos(\delta_n) \rceil \sin\left(\delta_n\right)\right]\right)^2$ by including the $\lceil \cos(\delta_k) \rceil$ and $\lceil \cos(\delta_l) \rceil$ terms. Due to the symmetry in δ_n, $\left(\mathbb{E}\left[\lceil \cos(\delta_n) \rceil \sin\left(\delta_n\right)\right]\right)^2 = 0$, so that $E_{\mathrm{off}}^{\mathrm{on}}(R, K) = \left(\mathbb{E}\left[\lceil \cos(\delta_n) \rceil \cos\left(\delta_n\right)\right]\right)^2$. Now, with the PDF of δ_n given in Fig. 5, the expected value can be calculated as follows:

$$\begin{aligned} &\mathbb{E}\left[\lceil \cos(\delta_n) \rceil \cos\left(\delta_n\right)\right] \\ &= 2\left[\int_0^{\frac{R}{2(K-1)}} \lceil \cos(\delta_n) \rceil \cos(\delta_n) \frac{K}{2\pi}\, d\delta_n \right. \\ &\quad \left. + \int_{\frac{R}{2(K-1)}}^{\pi - R/2} \lceil \cos(\delta_n) \rceil \cos(\delta_n) \frac{1}{2\pi}\, d\delta_n \right] \end{aligned} \tag{50}$$

where in the first integral, $\lceil \cos(\delta_n) \rceil = 1$ as $\frac{R}{2(K-1)} < \frac{\pi}{2}$. Whereas, in the second integral, when $\pi - R/2 > \frac{\pi}{2}$, i.e., $R < \pi$, the upper limit of the integral should be updated as $\frac{\pi}{2}$ as $\lceil \cos(\delta_n) \rceil = 0$ when $|\delta_n| > \frac{\pi}{2}$. Therefore, (50) is rewritten as

$$\begin{aligned} &\mathbb{E}\left[\lceil \cos(\delta_n) \rceil \cos\left(\delta_n\right)\right] \\ &\quad = \mathbb{E}\left[\cos\left(\delta_n\right)\right] \end{aligned}$$

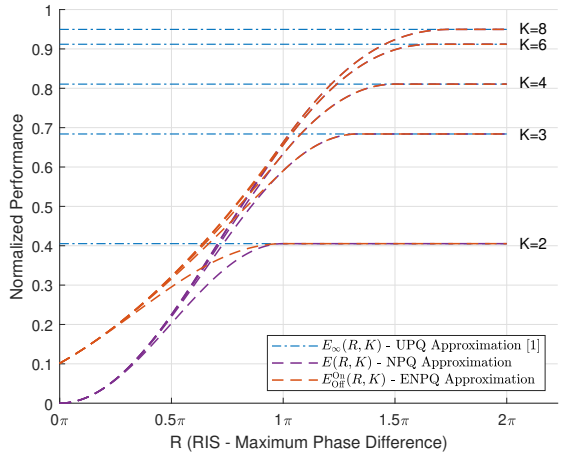

FIGURE 17: $E_{\text{off}}^{\text{on}}(R,K)$ vs R for $K \in \{2,3,4,6,8\}$

$$= 2\left[\int_0^{\frac{R}{2(K-1)}} \cos(\delta_n)\frac{K}{2\pi}\,d\delta_n + \int_{\frac{R}{2(K-1)}}^{\frac{\pi}{2}} \cos(\delta_n)\frac{1}{2\pi}\,d\delta_n\right]$$
$$= \frac{1}{\pi}\left[(K-1)\sin\left(\frac{R}{2(K-1)}\right)+1\right]. \quad (51)$$

where we keep the $\sin(\cdot)$ function instead of $\text{sinc}(\cdot)$ this time for a clearer notation. Thus, the approximation ratio for the ENPQ algorithm is

$$E_{\text{off}}^{\text{on}}(R,K) = \frac{1}{\pi^2}\left[(K-1)\sin\left(\frac{R}{2\pi(K-1)}\right)+1\right]^2. \quad (52)$$

An illustration for the theoretical calculations of the approximation $E_{\text{off}}^{\text{on}}(R,K)$ is given in Fig. 17, where it can be seen that $E_{\text{off}}^{\text{on}}(R,K)$ converges to the approximation ratio of the NPQ, i.e., $E(R,K)$, as R reaches π. We remark on the importance of using the ON/OFF β_n^r for $R<\pi$. This can be seen from Fig. 17 that as R approaches zero, while $E(R,K)$ becomes zero with all the elements being ON, $E_{\text{off}}^{\text{on}}(R,K)$ on the other hand becomes 0.1. Therefore, even with θ_n being the same for $n=1,\ldots,N$, i.e., no phase shifts selection as R becomes zero, ON/OFF selections solely could beat the performance of β_n^r for up to $K=8$ phase shift selections when $R<\pi/3$. Furthermore, when there are $K=2$ discrete phase shifts with ON/OFF β_n^r, the average performance is better than the case when $\beta_n^r=1$ with up to $K=8$ discrete phase shifts, for $R<2\pi/3$.

With NPQ and $R<\pi$, the normalized performance results are presented in Fig. 18 for $R=90°$, and in Fig. 19 for $R=150°$. As a validity check for our $E_{\text{off}}^{\text{on}}(R,K)$ calculation, we remark that the numerical results for ENPQ indeed converge to the theoretical approximation ratio. For a lower value of $R=90°$ in Fig. 18, the simple quantization approach with ON/OFF β_n^r selections outperforms the optimum solution with $\beta_n^r=1$ for $N\geq 100$. On the other hand, when R is high enough, say $R=150°$ as in Fig. 19, there is not such a loss due to the limited RIS phase range that ENPQ could exploit with ON/OFF β_n^r, resulting in Algorithm 1 being superior.

X. CONVERGENCE TO OPTIMALITY

We will now discuss the convergence of Algorithm 1 and Algorithm 2 to the optimal solution for $\beta_n^r=1$ and $\beta_n^r\in[0,1]$, $n=1,\ldots,N$, respectively. We know from *Lemma 1* and *Proposition 1* that Algorithm 1 will converge to the global optimum. Whereas, convergence to the global optimality of Algorithm 2 is guaranteed by *Lemma 2*, *Lemma 3*, *Proposition 1*, and *Proposition 2*. The required complexity is analyzed under two main components, which are the search complexity and the time complexity. The number of steps required will correspond to the search complexity. On the other hand, the number of complex vector additions will quantify the time complexity [20]. We remark that since $\theta_{n'}=\phi_{k'}$ in Step 6 of Algorithm 1 and in Step 15 of Algorithm 2, by using the Euler's formula, the term $h_{n'}\left(e^{j\theta_{n'}}-e^{j(\phi_{k'\ominus 1})}\right)$ can simply be expressed as $2h_{n'}\sin(\omega_{k'\ominus 1}/2)e^{j\left(\phi_{k'\ominus 1}+(\omega_{k'\ominus 1}+\pi)/2\right)}$. Therefore, each iteration of these algorithms will only incur one complex vector addition. Next, we will discuss the required complexity of both algorithms to achieve global optimality, individually.

First, for Algorithm 1, the **for** loop from Step 4 to Step 11 takes $\sum_{l=1}^{L}\mathcal{O}(|\mathcal{N}(\lambda_l)|)=\mathcal{O}(NK)$ steps. With this, one vector addition is performed for each updated element. Together with the N vector additions in Step 3, Algorithm 1 incurs $N(K+1)$ vector additions in total.

Second, for Algorithm 2, the **for** loop from Step 6 to Step 27 takes $\sum_{l=1}^{L'}\mathcal{O}(|\mathcal{N}(\lambda_l)|)=\mathcal{O}(N(K+1))$ steps. With this, there are $K+1$ arcs to be considered for each element, where only one vector addition is performed for each of those arcs. Together with the N vector additions in Step 5, Algorithm 2 incurs $N(K+2)$ vector additions in total. Note that, since the number of steps is larger for Algorithm 2, the required number of vector additions performed is also slightly larger than for Algorithm 1.

Finally, since in each step of both Algorithm 1 and Algorithm 2, only one or a small number of elements are updated, the time complexity of both algorithms will be linear in N. A detailed comparison with the recent literature is provided in the next section.

XI. PERFORMANCE AND COMPLEXITY COMPARISONS

In this section, we will discuss performance and complexity in a comparative way with the works from the literature. Firstly, to give a comparative trade-off between the presented algorithms in this paper, we present the performance results, i.e., 1st percentile SNR Boost [12], in Fig. 20, and complexity results, i.e., number of vector additions, in Fig. 21 for $K=2$. Moreover, in Fig. 20, we consider $R=90^o$ and $R=150^o$ to analyze the severe restriction and mild restriction on the RIS phase range, respectively, for $K=2$. In these results, we assume that the quantization algorithms will incur N

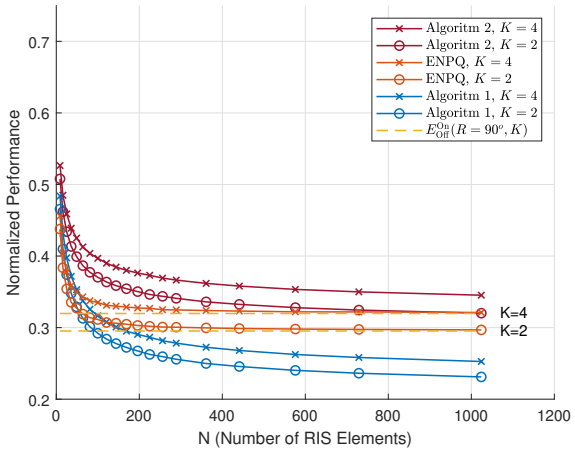

FIGURE 18: Normalized Performance results vs. N, for $R = 90°$ and $K \in \{2, 4\}$.

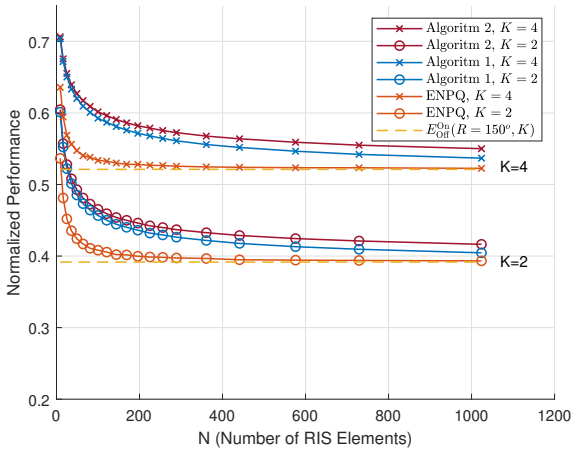

FIGURE 19: Normalized Performance results vs. N, for $R = 150°$ and $K \in \{2, 4\}$.

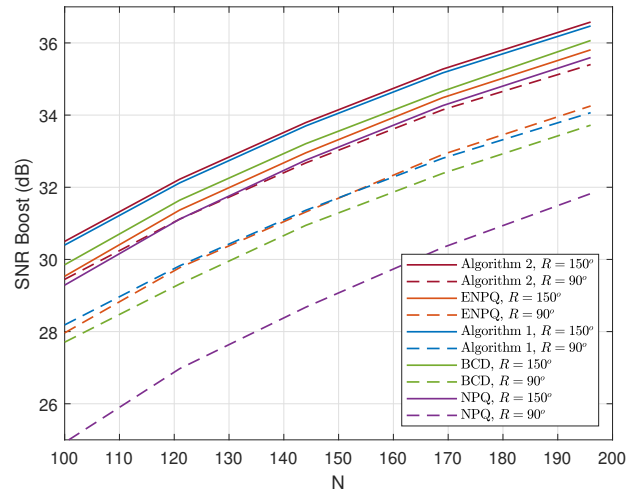

FIGURE 20: 1st percentile SNR Boost results vs. N, for $K = 2$ and $R \in \{90^o, 150^o\}$.

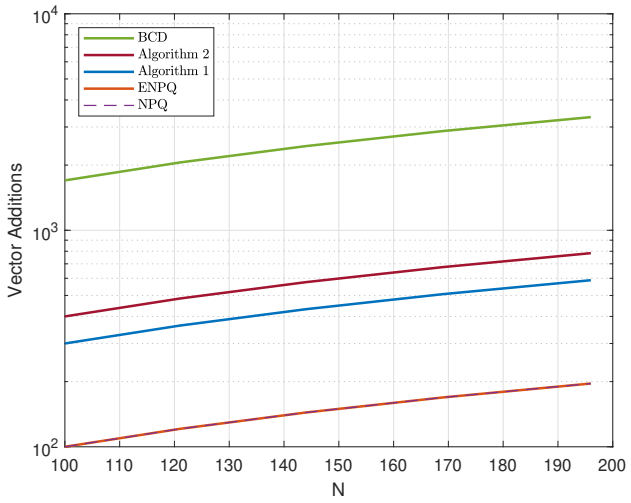

FIGURE 21: Time complexity results vs. N, for $K = 2$.

vector additions to produce the resulting SNR Boost value. Yet, even for the 1st percentile performance, ENPQ can perform surprisingly well while requiring lower complexity, especially for lower R. Regarding the comparison of the optimum algorithms and the quantization algorithms, we focus on Algorithm 2 versus ENPQ and Algorithm 1 versus NPQ. Algorithm 2 incurs four times the vector additions required by ENPQ while providing about 1 dB and 2 dB gain for $R = 150^o$ and $R = 90^o$, respectively. On the other hand, Algorithm 1 incurs three times the vector additions required by NPQ yet can provide more than 3 dB gain for $R = 90^o$. This additional gain that Algorithm 1 can provide vanishes for larger R. Finally, in Fig. 20, BCD can provide more performance than NPQ and ENPQ for $R \in \{90^o, 150^o\}$ and $R = 150^o$, respectively. However, it comes with a significant jump in complexity.

Regarding the comparisons with the literature, as we discussed in Section I, the works that deal with the exact problem introduced in this paper, i.e., the nonuniform discrete phase shifts and RIS phase range restriction, are not extensive, being restricted to [20]–[22]. Therefore, we will provide a discussion as to the comparative performance of this work with those from the literature, i.e., [20]–[22].

A. PERFORMANCE COMPARISON WITH THE LITERATURE

The work in this paper is an extension of [19] in that the problem is the same power maximization one but the phase range R is less than 2π, the discrete phase shifts set Φ_K can

be arbitrary, and the RIS gains $\beta_n^r \in [0,1]$ can be adjustable. We first show that the same set of necessary and sufficient conditions apply to the problem with the limited phase range when $\beta_n^r = 1$ for $n = 1, 2, \ldots, N$ and we develop new conditions on the optimality when $\beta_n^r \in [0,1]$. Assuming $\beta_n^r = 1$ for $n = 1, 2, \ldots, N$, we developed an *optimal* algorithm, Algorithm 1, an extension of [19, Algorithm 1], as well as a suboptimal algorithm called NPQ. For $\beta_n^r \in [0,1]$, using the new conditions on the optimality, we developed another *optimal* algorithm, Algorithm 2, as an extension of Algorithm 1 in this paper for $R < \pi$, as well as a novel suboptimal algorithm called ENPQ. Simulation results show that the performance results of Algorithm 1 and NPQ, or similarly Algorithm 2 and ENPQ, for single-input single-output (SISO) systems are close, especially for large N. We remark that the algorithms in this paper cover a wide range of scenarios regarding discrete beamforming optimization with RISs, e.g., RIS phase range restriction, adjustable RIS gains, and arbitrarily selected nonuniform discrete phase shifts.

The work in [20] attempts to maximize the capacity in the channel from the BS to the UE via the RIS, where they only consider $R < \pi$. Since it claims global optimality, the performance would be the same as Algorithm 2 for $R < \pi$, but, we will see in the next subsection that Algorithm 2 will require significantly fewer number of complex vector additions. With this, the work in [20] compares its capacity results with that of CPP, a suboptimal algorithm similar to NPQ. However, our novel algorithm ENPQ is more competitive against Algorithm 2 than NPQ for $R < \pi$, e.g., in Fig. 18, and in [20] this kind of analysis is not present as they only compare with CPP, which does not perform well when $R < \pi$. Reference [21] tries to maximize Long-Term Average Received Power (LARP), where the average is taken in the statistical sense via an expectation operator. This paper provides simulation results in terms of a number of channel models, i.e., Rician, Rayleigh, and pure LOS fading. Performance results for LARP are provided in [21, Fig. 4] for the three fading models for RIS sizes of 1–10^4 elements employing continuous phase shifts. There are other simulation results provided, such as LARP against decrement of phase shifting capability, incident angle, phase shifting capacity, or control voltage. However, [21] does not have a result we can use to compare with ours. And, unlike this work, [21] does not provide an indication of what the theoretical maximum gain in LARP is. Neither does it have a similar result to our necessary and sufficient conditions for global optimality. Reference [22] studies the problem of minimizing the transmit power at the BS while the received power is above a certain threshold. It can be considered as the extension of divide-and-sort (DaS) search algorithm proposed in [25] for *uniform* discrete phase shifts and it can be perhaps interpreted as the dual of our received power maximization problem. Reference [22] proposes an algorithm called partition-and-traversal (PAT) for that purpose. Reference [22] claims to ensure global optimality and shows a perfect fit with exhaustive search results for RIS elements up to 50 in [22, Fig. 4]. In addition, [22] discusses two suboptimal algorithms, which are manifold optimization (Manopt) and semidefinite relaxation-semidefinite program (SDR-SDP). We remark that in [22], RIS gains are set to be always ON for the sake of optimization. Yet, in this work, our extensive analysis shows the importance of ON/OFF selections when $R < \pi$, and this kind of analysis is missing in [22]. In [22, Fig. 7], the performance of PAT, exhaustive search, Manopt, and SDR are depicted. Since the PAT claims global optimality, it would give the same performance as Algorithm 1. With this, neither Manopt nor SDR comes any close to the performance of NPQ as suboptimal algorithms. Yet, we remark that Algorithm 2 is guaranteed to perform better than PAT whenever $R < \pi$ and ENPQ can also perform better than PAT when, for example, $R = 90^o$ as shown in Fig. 18.

Table 1: Comparison of Algorithms 1-2 and NPQ-ENPQ with algorithms from the literature.

	Search Steps	Time Complexity	Optimality Guarantee
[12] CPP	Projection of Phase Selections	—	Local
[20] PBO	$N(K+1)$	$\mathcal{O}(N(2K+3))$	Global For $R < 180^o$
[21] GBQ	$\frac{K(K-1)}{2} + N$	$\approx \mathcal{O}(N)$ $(N \gg K)$	Local
[22] PAT	$2NK$ (SISO)	—	Global, $R \geq 180^o$ Local, $R < 180^o$
NPQ	Deterministic	—	Local For $R \geq 180^o$
ENPQ	Deterministic	—	Local For $R < 180^o$
Algo. 1	$\leq \boldsymbol{NK}$	$\mathcal{O}(N(K+1))$	Global For $R \geq 180^o$
Algo. 2	$\leq \boldsymbol{N(K+1)}$	$\mathcal{O}(N(K+2))$	Global For $R < 180^o$

B. COMPLEXITY COMPARISON WITH THE LITERATURE

Among [20]–[22] from the literature that deal with the same problem considered in this paper, only [20] and [22] claim global optimality. Hence, we compare the complexity of our optimum algorithms with these references. We remark that the solution for the same problem using uniformly distributed discrete phase shifts requires significantly less complexity. A detailed complexity analysis for the uniform case is provided in [19]. Now, we will carry out the complexity analysis for the nonuniform case in three main components: The sorting requirement, the number of search steps required, and the number of complex vector additions. While the number

of search steps corresponds to the search space size, the number of complex vector additions will represent the overall computational time complexity.

Firstly, the algorithms work with the sorted s_{nk} according to their arguments, i.e., the update rule $\mathcal{N}(\lambda_l)$ requires sorting. The sorting enables *elementwise* updates between the search steps to achieve linear time complexity, which was mostly ignored by the literature when solving the problem with uniform discrete phase shifts [19]. The same requirement persists with the nonuniform phase shits. Assuming λ_l are uniformly distributed, the sorting in $\mathcal{N}(\lambda_l)$ will take $\mathcal{O}(N)$ time on average [14]. Besides this, more generally, to sort the $L \leq NK$ or $L^{'} \leq N(K+1)$ arguments in the update rules of Algorithm 1 and Algorithm 2, traditional sorting algorithms may require $\mathcal{O}(L\log(L))$ and $\mathcal{O}(L^{'}\log(L^{'}))$ complexity for Algorithm 1 and Algorithm 2, respectively. We remark that the authors in [20] develop a special sorting algorithm that can work with complexity $\mathcal{O}(N(K+1)\log(K+1))$, however, it is assumed that the sorting of the cascaded channel phases would be readily provided, i.e., α_n are assumed to be sorted.

Secondly, the number of search steps required to ensure global optimality should be considered. In this paper, our algorithms consider repetitions among s_{nk} and have the potential to reduce the search steps further, i.e., $L \leq NK$ and $L \leq N(K+1)$ for Algorithm 1 and Algorithm 2, respectively. In [20], the required number of steps is fixed to $N(K+1)$, which is more than or the same as Algorithm 2 and is not reduced for $R \geq \pi$. In [22], the complexity analysis is provided in terms of the search space size only, where the proposed PAT algorithm would incur $2NK$ steps for the special case of SISO. In [22, Fig. 5], the plot for the SISO scenario shows around 7 dB increase in the search space for increasing the number of elements from 20 to 100. Since $10\log(100/20) \approx 7$ dB, this would correspond to a linear complexity in the number of elements.

Finally, the number of vector additions required by our algorithms is $N(K+1)$ when $R \geq \pi$ and $N(K+2)$ when $R < \pi$, i.e., for Algorithm 1 and Algorithm 2, respectively. In [20], the proposed partitioning based optimization (PBO) requires $N(2K+3)$ complex vector additions. Consequently, PBO incurs at least $N(K+1)$ extra vector additions compared to our algorithms, with the number of extra additions increasing linearly with both the number of RIS elements and the number of discrete phase shifts.

We summarize the performance comparisons in Table 1 for clarity. While the focus was on the optimal algorithms in this section, the suboptimal algorithms are also presented in Table 1.

XII. EXTENSION TO THE MULTIUSER SCENARIO

In the literature, ample research on RIS deals with multiple users, where the problem is generally formulated as an optimization problem to maximize the overall throughput [26], [27], or similarly the sum rate [28]–[31]. These approaches commonly consider inter-user interference. In [26], the authors investigate the joint beamforming problem for a multiuser SISO communication aided by an active RIS. Reference [27] maximizes the throughput of an RIS-assisted UAV-to-ground user communications while simultaneously minimizing the average total power consumption, where the RIS is assumed to have continuous phase shifts. From the perspective of sum rate maximization, the sum of weighted rates is maximized with successive convex approximation in [28], the sum rate is maximized in [29] via joint beamforming for the BS and an RIS with discrete phase shifts, achievable sum rate maximization is performed while the RIS uses continuous phase shifts in [30], and the authors in [31] maximize the sum rate by eliminating the inter-user-interference with the assumption of zero force precoding at the BS and continuous phase shifts at the RIS. Moreover, the problem of maximizing the minimum SNR among multiple users has also drawn significant attention from the recent literature, with continuous [32], [33], and discrete phase shifts [34]–[37]. In [32], the authors consider maximizing the minimum of the achievable rates of the users given SNR, whereas, in [33], the max-min beamforming gain is achieved based on matrix lifting and linear matrix inequality techniques. For the max-min SNR problem with discrete phase RISs, SDR and gradient descent/ascent (GDA) approaches are used in [34], BCD is used in [35] for passive beamforming, and a blind beamforming approach is developed in both [36] and [37] based on the received power data. In these works, the optimization problems are naturally NP-hard and global optimality is hard to achieve with discrete phase RISs. Therefore, results are mostly approximations and sub-optimal.

RIS partitioning has also drawn attention as an alternative approach to the aforementioned solutions. The main idea is to partition the RIS into multiple groups of elements, where a certain group serves a single user [38]–[42]. It is shown in [42] that the interference among other groups of elements in a multiuser scenario can be neglected when the RIS is a uniform linear array. So, the multiuser problem can boil down to optimizing an RIS partition for a single user, which is a motivating factor to study the single-user problem [20], as we did in this paper.

We extend our results for a multicast network, assuming perfect channel state information (CSI), similar to the scenarios considered in [12], [14], [19]. Consider a max-min SNR problem with $U \geq 2$ receivers with a transmit power of $P = 30$ dBm, i.e.,

$$\max_{\theta_n \in \Phi_K} \min_{u} \left\{ \frac{P|\beta_{0,u}e^{j\alpha_{0,u}} + \sum_{n=1}^{N} \beta_{n,u}e^{j(\alpha_{n,u}+\theta_n)}|^2}{\sigma_u^2} \right\}, \tag{53}$$

where $\sigma_u^2 = -90$ dBm is the noise variance at each receive antenna, $h_{0,u} = \beta_{0,u}e^{j\alpha_{0,u}}$ is the direct channel, and $h_{n,u} = \beta_{n,u}e^{j\alpha_{n,u}}$ is the reflected channel through the n-th RIS element for the u-th receiver.

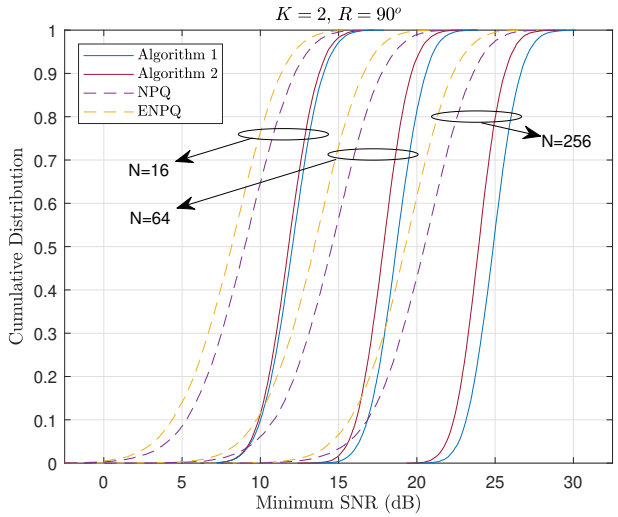

FIGURE 22: CDF of the minimum SNR across $U = 4$ users for $K = 2$, $N \in \{16, 64, 256\}$, and $R = 90^o$.

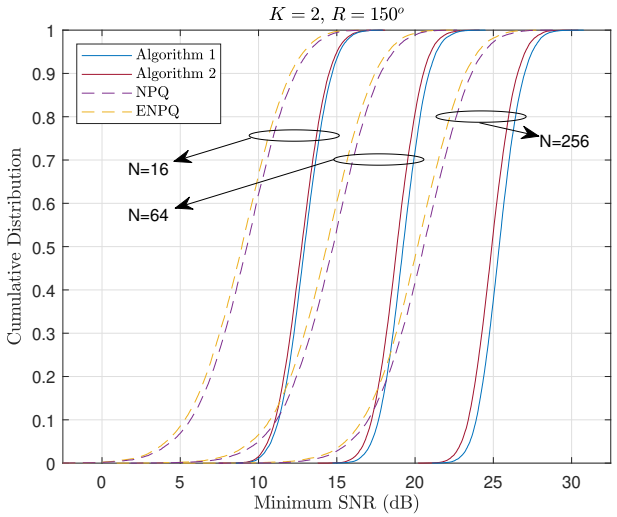

FIGURE 23: CDF of the minimum SNR across $U = 4$ users for $K = 2$, $N \in \{16, 64, 256\}$, and $R = 150^o$.

The way we extend our algorithms is as follows. For NPQ and ENPQ, each algorithm is repeated for each user, then the RIS configuration that maximizes the minimum SNR among the users is selected. On the other hand, while performing Algorithm 1–2 for user u, we decide the best possible solution in the **for** loop of Algorithm 1–2 by maximizing the minimum channel gain among all users. Therefore, Algorithm 1 and Algorithm 2 incur $NU(K+1)$ and $NU(K+2)$ vector additions, respectively. Then, this process is repeated for each user, to select the best option among U possibilities, which results in $\mathcal{O}(NU^2(K+1))$ and $\mathcal{O}(NU^2(K+2))$ time complexity in total for Algorithm 1 and Algorithm 2. We remark that NPQ and ENPQ algorithms will also require vector additions unlike the single-user scenario, because we need to search for the maximum available powers. Therefore, both suboptimal algorithms will result in $\mathcal{O}(NU^2)$ time complexity.

The CDF plots for the minimum SNR performance of the multicast extension are given in Fig. 22 and Fig. 23 for $R = 90^o$ and $R = 150^o$, respectively when $K = 2$ and $N \in \{16, 64, 256\}$. The results show that both Algorithm 1 and NPQ with the always ON approach perform better than their extended versions with ON/OFF consideration when $R < \pi$. This difference gets smaller for larger R since these pair of algorithms would provide the same outcome, as given in Fig. 15. Overall, it can be seen that Algorithm 1 can provide superior performance compared to the quantization approach, i.e., NPQ. When $R = 90^o$, the average gain of Algorithm 1 against NPQ is 3.0 dB for $N = 16$ and 4.4 dB for $N = 256$. When $R = 150^o$, the average gain of Algorithm 1 against NPQ is 3.6 dB for $N = 16$ and about 5.0 dB for $N = 256$. Therefore, considering the complexity jump in the quantization approach for the multiuser extension, our optimal algorithm can become an even better option. Note that these gains with Algorithm 1 get larger as N increases.

XIII. CONCLUSION

In this paper, to maximize the received power at a UE, we provided necessary and sufficient conditions for determination of the RIS coefficients that are subject to nonuniform discrete phase shifts. We employed these conditions to achieve the optimum solution in linear time and with less complexity than the existing solutions in the literature. Also, we established a foundation on the RIS phase range R with the nonuniform discrete phase shifts structure. We proved that the optimum placement of the nonuniform discrete phase shifts would be equally separated over the RIS phase range. Then, we showed that whenever $R < \pi$, adjusting RIS gains can bring significant performance, and the globally optimum solution would be yielded by the RIS elements being either ON or OFF.

In addition to the optimum algorithms, we also calculated the approximation ratio for the nonuniform discrete phase shifts by employing the intuitive quantization algorithm. Furthermore, with the ON/OFF RIS gains, we proposed a novel quantization algorithm named ENPQ, a low-complexity algorithm that can bring significant performance when there is a notable limitation in the RIS phase range, with which we also provided a secondary closed-form solution for the approximation ratio for nonuniform discrete phase shifts.

REFERENCES

[1] E. Basar, M. Di Renzo, J. De Rosny, M. Debbah, M.-S. Alouini, and R. Zhang, "Wireless communications through reconfigurable intelligent surfaces," *IEEE Access*, vol. 7, pp. 116 753–116 773, 2019.

[2] E. Ayanoglu, F. Capolino, and A. L. Swindlehurst, "Wave-controlled metasurface-based reconfigurable intelligent surfaces," *IEEE Wireless Communications*, May 2022.

[3] E. Björnson, H. Wymeersch, B. Matthiesen, P. Popovski, L. Sanguinetti, and E. de Carvalho, "Reconfigurable intelligent surfaces: A signal processing perspective with wireless applications," *IEEE Signal Processing Magazine*, vol. 39, no. 2, pp. 135–158, Feb. 2022.

[4] X. Pei, H. Yin, L. Tan, L. Cao, Z. Li, K. Wang, K. Zhang, and E. Björnson, "RIS-aided wireless communications: Prototyping, adaptive beamforming, and indoor/outdoor field trials," *IEEE Transactions on Communications*, vol. 69, no. 12, pp. 8627–8640, Sep. 2021.

[5] X. Yu, D. Xu, and R. Schober, "Enabling secure wireless communications via intelligent reflecting surfaces," in *2019 IEEE Global Communications Conference (GLOBECOM)*, 2019, pp. 1–6.

[6] Q. Wu and R. Zhang, "Intelligent reflecting surface enhanced wireless network via joint active and passive beamforming," *IEEE Transactions on Wireless Communications*, vol. 18, no. 11, pp. 5394–5409, 2019.

[7] X. Yu, D. Xu, and R. Schober, "Optimal beamforming for MISO communications via intelligent reflecting surfaces," in *2020 IEEE 21st International Workshop on Signal Processing Advances in Wireless Communications (SPAWC)*, 2020, pp. 1–5.

[8] X. Qian, M. Di Renzo, J. Liu, A. Kammoun, and M.-S. Alouini, "Beamforming through reconfigurable intelligent surfaces in single-user mimo systems: Snr distribution and scaling laws in the presence of channel fading and phase noise," *IEEE Wireless Communications Letters*, vol. 10, no. 1, pp. 77–81, 2021.

[9] Q. Wu and R. Zhang, "Beamforming optimization for wireless network aided by intelligent reflecting surface with discrete phase shifts," *IEEE Transactions on Communications*, vol. 68, no. 3, pp. 1838–1851, Dec. 2019.

[10] Z. Yigit, E. Basar, and I. Altunbas, "Low complexity adaptation for reconfigurable intelligent surface-based MIMO systems," *IEEE Communications Letters*, vol. 24, no. 12, pp. 2946–2950, 2020.

[11] C. You, B. Zheng, and R. Zhang, "Channel estimation and passive beamforming for intelligent reflecting surface: Discrete phase shift and progressive refinement," *IEEE Journal on Selected Areas in Communications*, vol. 38, no. 11, pp. 2604–2620, 2020.

[12] Y. Zhang, K. Shen, S. Ren, X. Li, X. Chen, and Z.-Q. Luo, "Configuring intelligent reflecting surface with performance guarantees: Optimal beamforming," *IEEE Journal of Selected Topics in Signal Processing*, vol. 16, no. 5, pp. 967–979, Aug. 2022.

[13] R. Xiong, X. Dong, T. Mi, K. Wan, and R. C. Qiu, "Optimal discrete beamforming of RIS-aided wireless communications: An inner product maximization approach," arXiv:2211.04167v6, Nov. 2023.

[14] S. Ren, K. Shen, X. Li, X. Chen, and Z.-Q. Luo, "A linear time algorithm for the optimal discrete IRS beamforming," *IEEE Wireless Communications Letters*, vol. 12, no. 3, pp. 496–500, Mar. 2023.

[15] M. Jung, W. Saad, M. Debbah, and C. S. Hong, "On the optimality of reconfigurable intelligent surfaces (RISs): Passive beamforming, modulation, and resource allocation," *IEEE Transactions on Wireless Communications*, vol. 20, no. 7, pp. 4347–4363, 2021.

[16] J. Luo, K. Pattipati, and P. Willett, "A sub-optimal soft decision PDA method for binary quadratic programming," in *2001 IEEE International Conference on Systems, Man and Cybernetics. e-Systems and e-Man for Cybernetics in Cyberspace (Cat.No.01CH37236)*, vol. 5, 2001, pp. 3140–3145 vol.5.

[17] A. Yellepeddi, K. J. Kim, C. Duan, and P. Orlik, "On probabilistic data association for achieving near-exponential diversity over fading channels," in *2013 IEEE International Conference on Communications (ICC)*, 2013, pp. 5409–5414.

[18] A. Pradhan and H. S. Dhillon, "A probabilistic reformulation technique for discrete RIS optimization in wireless systems," *IEEE Transactions on Wireless Communications*, pp. 1–1, 2023.

[19] D. K. Pekcan and E. Ayanoglu, "Achieving optimum received power for discrete-phase RISs with elementwise updates in the least number of steps," *IEEE Open Journal of the Communications Society*, vol. 5, pp. 2706–2722, 2024.

[20] S. Hashemi, H. Jiang, and M. Ardakani, "Optimal configuration of reconfigurable intelligent surfaces with arbitrary discrete phase shifts," *IEEE Transactions on Communications*, to be published (available as Early Access paper from *IEEE Xplore*).

[21] L. T. L. Cao, H. Yin and X. Pei, "RIS with insufficient phase shifting capability: Modeling, beamforming, and experimental validations," *IEEE Transactions on Communications*, to be published (available as Early Access paper from *IEEE Xplore*).

[22] J. Lu, R. Xiong, T. Mi, K. Yin, and R. C. Qiu, "Optimal configuration of reconfigurable intelligent surfaces with non-uniform phase quantization," arXiv preprint arXiv:2405.06967, May 2024.

[23] B. Rana, S.-S. Cho, and I.-P. Hong, "Review paper on hardware of reconfigurable intelligent surfaces," *IEEE Access*, vol. 11, pp. 29 614–29 634, 2023.

[24] S. Abeywickrama, R. Zhang, Q. Wu, and C. Yuen, "Intelligent reflecting surface: Practical phase shift model and beamforming optimization," *IEEE Transactions on Communications*, vol. 68, no. 9, pp. 5849–5863, 2020.

[25] R. Xiong, X. Dong, T. Mi, K. Wan, and R. C. Qiu, "Optimal discrete beamforming of RIS-aided wireless communications: An inner product maximization approach," in *2024 IEEE Wireless Communications and Networking Conference (WCNC)*, 2024, pp. 1–6.

[26] P. Zeng, D. Qiao, Q. Wu, and Y. Wu, "Throughput maximization for active intelligent reflecting surface-aided wireless powered communications," *IEEE Wireless Communications Letters*, vol. 11, no. 5, pp. 992–996, 2022.

[27] L. Gu and A. Mohajer, "Joint throughput maximization, interference cancellation, and power efficiency for multi-irs-empowered uav communications," *Signal, Image and Video Processing*, vol. 18, no. 5, pp. 4029–4043, 2024.

[28] Y. Pan, K. Wang, C. Pan, H. Zhu, and J. Wang, "Uav-assisted and intelligent reflecting surfaces-supported terahertz communications," *IEEE Wireless Communications Letters*, vol. 10, no. 6, pp. 1256–1260, 2021.

[29] B. Di, H. Zhang, L. Li, L. Song, Y. Li, and Z. Han, "Practical hybrid beamforming with finite-resolution phase shifters for reconfigurable intelligent surface based multi-user communications," *IEEE Transactions on Vehicular Technology*, vol. 69, no. 4, pp. 4565–4570, 2020.

[30] W. Yan, X. Yuan, Z.-Q. He, and X. Kuai, "Passive beamforming and information transfer design for reconfigurable intelligent surfaces aided multiuser mimo systems," *IEEE Journal on Selected Areas in Communications*, vol. 38, no. 8, pp. 1793–1808, 2020.

[31] J.-S. Jung, C.-Y. Park, J.-H. Oh, and H.-K. Song, "Intelligent reflecting surface for spectral efficiency maximization in the multi-user miso communication systems," *IEEE Access*, vol. 9, pp. 134 695–134 702, 2021.

[32] Q. Huang, J. Hu, Q. Yue, and K. Yang, "Beamforming design in intelligent reflecting surface aided multicast system in ultra-high frequency bands with large-scale antenna array," *IEEE Wireless Communications Letters*, vol. 13, no. 5, pp. 1429–1433, 2024.

[33] W. Ma, L. Zhu, and R. Zhang, "Passive beamforming for 3-d coverage in irs-assisted communications," *IEEE Wireless Communications Letters*, vol. 11, no. 8, pp. 1763–1767, 2022.

[34] G. Yan, L. Zhu, and R. Zhang, "Passive reflection optimization for irs-aided multicast beamforming with discrete phase shifts," *IEEE Wireless Communications Letters*, vol. 12, no. 8, pp. 1424–1428, 2023.

[35] A. Al-Hilo, M. Samir, M. Elhattab, C. Assi, and S. Sharafeddine, "Reconfigurable intelligent surface enabled vehicular communication: Joint user scheduling and passive beamforming," *IEEE Transactions on Vehicular Technology*, vol. 71, no. 3, pp. 2333–2345, 2022.

[36] F. Xu, J. Yao, W. Lai, K. Shen, X. Li, X. Chen, and Z.-Q. Luo, "Blind beamforming for coverage enhancement with intelligent reflecting surface," *IEEE Transactions on Wireless Communications*, pp. 1–1, 2024.

[37] W. Lai, W. Wang, F. Xu, X. Li, S. Niu, and K. Shen, "Adaptive blind beamforming for intelligent surface," *IEEE Transactions on Mobile Computing*, pp. 1–17, 2024.

[38] A. Khaleel and E. Basar, "A novel noma solution with ris partitioning," *IEEE Journal of Selected Topics in Signal Processing*, vol. 16, no. 1, pp. 70–81, 2022.

[39] M. Makin, S. Arzykulov, A. Celik, A. M. Eltawil, and G. Nauryzbayev, "Optimal ris partitioning and power control for bidirectional noma networks," *IEEE Transactions on Wireless Communications*, vol. 23, no. 4, pp. 3175–3189, 2024.

[40] C. You, B. Zheng, W. Mei, and R. Zhang, "How to deploy intelligent reflecting surfaces in wireless network: Bs-side, user-side, or both sides?" *Journal of Communications and Information Networks*, vol. 7, no. 1, pp. 1–10, 2022.

[41] M. Aldababsa, A. Khaleel, and E. Basar, "Simultaneous transmitting and reflecting reconfigurable intelligent surfaces-empowered noma networks," *IEEE Systems Journal*, vol. 17, no. 4, pp. 5441–5451, 2023.

[42] Y. Kim, J.-H. Kim, and C.-B. Chae, "Partition-based ris-assisted multiple access: Noma decoding order perspective," *IEEE Transactions on Vehicular Technology*, vol. 71, no. 8, pp. 9083–9088, 2022.

DOGAN KUTAY PEKCAN (Graduate Student Member, IEEE) received his B.S. and M.S. degrees in Electrical and Electronics Engineering from Bilkent University, Ankara, Türkiye, in 2018 and 2021, respectively. During his M.S. studies, he worked on research and development of detection and estimation algorithms, for various 5G physical layer channels, specializing in channel estimation and phase noise mitigation in mm-Wave. Currently, he is pursuing his Ph.D. degree in Electrical Engineering and Computer Science at University of California, Irvine, CA, USA. His research interests include wireless communications, reconfigurable intelligent surfaces, and algorithms.

HONGYI LIAO (Graduate Student Member, IEEE) received the B.Eng. degree in Electrical Engineering and Automation from Sichuan University, Sichuan, China, in 2020. He is currently pursuing the M.S. degree in Electrical Engineering and Computer Science at University of California, Irvine, CA, USA. His research interests include wireless communications, reconfigurable intelligent surfaces, and optimization algorithms.

ENDER AYANOGLU (Fellow, IEEE) received the Ph.D. degree in electrical engineering from Stanford University, Stanford, CA, USA, in 1986. He was with the Bell Laboratories Communications Systems Research Laboratory, Holmdel, NJ, USA. From 1999 to 2002, he was a Systems Architect with Cisco Systems Inc., San Jose, CA. Since 2002, he has been a Professor with the Department of Electrical Engineering and Computer Science, University of California, Irvine, CA, where he was the Director of the Center for Pervasive Communications and Computing and the Conexant-Broadcom Endowed Chair, from 2002 to 2010. He was a recipient of the IEEE Communications Society Stephen O. Rice Prize Paper Award in 1995, the IEEE Communications Society Best Tutorial Paper Award in 1997, and the IEEE Communications Society Communication Theory Technical Committee Outstanding Service Award in 2014. From 2000 to 2001, he was the Founding Chair of the IEEE-ISTO Broadband Wireless Internet Forum, an industry standards organization. He served on the Executive Committee for the IEEE Communications Society Communication Theory Committee, from 1990 to 2002, and its Chair, from 1999 to 2002. From 1993 to 2014, he was an Editor of IEEE TRANSACTIONS ON COMMUNICATIONS. He was the Editor-in-Chief of IEEE TRANSACTIONS ON COMMUNICATIONS, from 2004 to 2008, and the IEEE JOURNAL ON SELECTED AREAS IN COMMUNICATIONS-Series on Green Communications and Networking, from 2014 to 2016. He was the Founding Editor-in-Chief of IEEE TRANSACTIONS ON GREEN COMMUNICATIONS AND NETWORKING, from 2016 to 2020. He served as an IEEE Communications Society Distinguished Lecturer, from 2022 to 2023 and will serve in the same capacity in 2024-2025. In 2023, he received the IEEE Communications Society Joseph LoCicero Award for outstanding contributions to IEEE Communications Society journals as Editor, Editor-in-Chief (EiC), and Founding EiC.